JOC
The Journal of Organic Chemistry
JULY 5, 2013 VOLUME 78, NUMBER 13 pubs.acs.org/joc

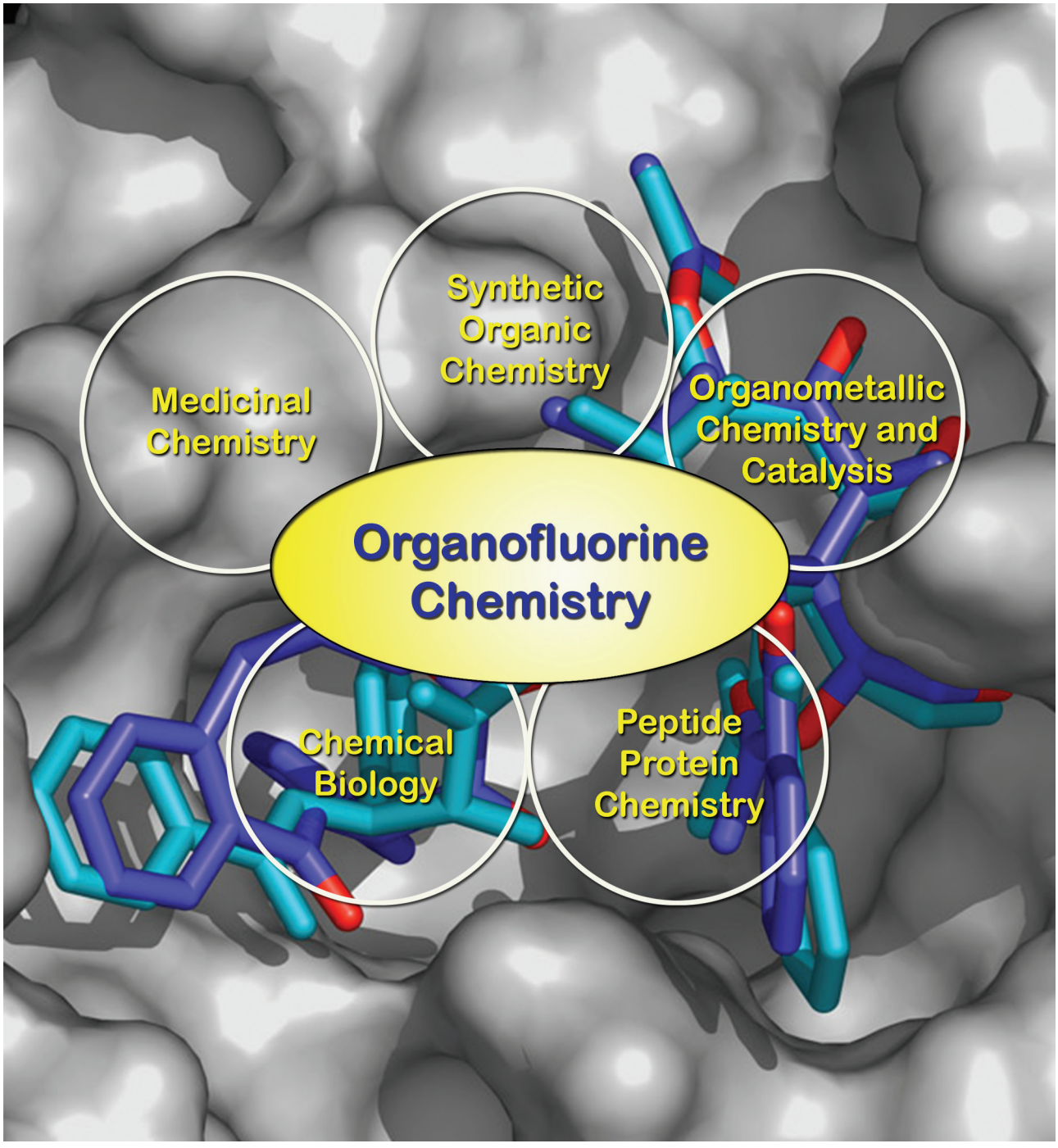

ACS Publications
MOST TRUSTED. MOST CITED. MOST READ.
www.acs.org

About the Cover:

Research endeavors are represented on the exploration of organofluorine chemistry at the multidisciplinary interface of biology and chemistry. The background is the tubulin-bound "REDOR–Taxol" molecule and a macrocyclic analog mimicking it at the β-tubulin binding site for Taxol. See Ojima, 6358. Professor Iwao Ojima is the recipient of the 2013 ACS Award for Creative Work in Fluorine Chemistry. View the article.

JOC The Journal of Organic Chemistry

Perspective

pubs.acs.org/joc

Exploration of Fluorine Chemistry at the Multidisciplinary Interface of Chemistry and Biology

Iwao Ojima*

Department of Chemistry and Institute of Chemical Biology & Drug Discovery, Stony Brook University, Stony Brook, New York 11794-3400, United States

ABSTRACT: Over the last three decades, my engagement in "fluorine chemistry" has evolved substantially because of the multidisciplinary nature of the research programs. I began my research career as a synthetic chemist in organometallic chemistry and homogeneous catalysis directed toward organic synthesis. Then, I was brought into a very unique world of "fluorine chemistry" in the end of 1970s. I started exploring the interface of fluorine chemistry and transition metal homogeneous catalysis first, which was followed by amino acids, peptides, and peptidomimetics for medicinal chemistry. Since then, I have been exploring the interfaces of fluorine chemistry and multidisciplinary fields of research involving medicinal chemistry, chemical biology, cancer biology, and molecular imaging. This perspective intends to cover my fruitful endeavor in the exploration of fluorine chemistry at the multidisciplinary interface of chemistry and biology in a chronological order to show the evolution of my research interest and strategy.

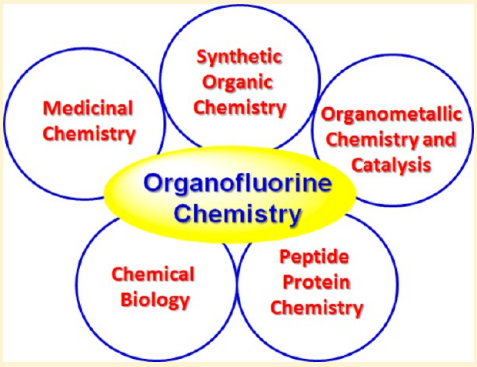

INTRODUCTION

The extraordinary potential of fluorine-containing biologically relevant molecules in peptide/protein chemistry, medicinal chemistry, chemical biology, pharmacology, drug discovery as well as diagnostic and therapeutic applications was recognized by researchers who are not in the traditional fluorine chemistry field, and thus a new wave of fluorine chemistry has been rapidly expanding its biomedical frontiers. In fact, the importance of fluorine in bioorganic and medicinal chemistry has been demonstrated by a large number of fluorinated compounds approved by the FDA for medical use.[1−3] According to our survey in 2008, 138 fluorine-containing drugs have received FDA approval for human diseases (of which 23, however, have been discontinued from the market), while 33 are currently in use for veterinary applications.[4] These statistics make fluorine the "second-favorite heteroatom" after nitrogen in drug design.

Small atomic radius, high electronegativity, nuclear spin of 1/2, and low polarizability of the C−F bond are among the special properties that render fluorine so attractive. These atomic properties translate widely into equally appealing attributes of fluoroorganic compounds. Higher metabolic stability, often increased binding to target molecules, and increased lipophilicity and membrane permeability are some of the properties associated with the replacement of a C−H or C−O bond with a C−F bond in biologically active compounds. Because of the recognized value of fluorine, it is now a common practice in drug discovery to study fluoro-analogues of lead compounds under development. It should be noted that in 2006 the best and the second best selling drugs in the world were Lipitor (atorvastatin calcium) (by Pfizer/Astellas; $14.4 billion/year) and Advair (USA)/seretide(EU) (a mixture of fluticasone propionate and salmeterol) (by GlaxoSmithKline; $6.1 billion/year), which contain one and three fluorine atoms, respectively.[5] These huge successes of fluorine-containing drugs keep stimulating research on fluorine in medicinal chemistry for drug discovery. As such, it is not an exaggeration to say that every new drug discovery and development today explores fluorine-containing drug candidates without exception.

Although medicinal chemists have been introducing fluorine into bioactive molecules on the basis of experience and intuition, it is only recently that experimental and computational studies have been conducted to better understand how the introduction of fluorine into small drug molecules results in higher binding affinities and selectivity.[6] An understanding of how the replacement of H with F affects the electronic nature and conformation of small molecules is crucial for predicting the interaction of fluoroorganic molecules with proteins and enzymes. In addition, ^{19}F NMR has found numerous applications to molecular imaging and promoted the development of molecular probes for imaging. The sensitivity of ^{19}F NMR spectroscopy, along with large ^{19}F−^{1}H coupling constants and the virtual absence of ^{19}F in living tissues, makes incorporation of fluorine into bioactive compounds a particularly powerful tool for the investigation of biological processes.[7−9] Also, applications of ^{18}F-PET (positron emission tomography), a powerful in vivo imaging technology in oncology, neurology, psychiatry, cardiology, and other medical specialties, have already become an essential part of medical care. In addition, ^{18}F-PET has emerged as an important tool in

Received: February 8, 2013
Published: April 24, 2013

   dx.doi.org/10.1021/jo400301u | J. Org. Chem. 2013, 78, 6358−6383

drug development, especially for accurate measurements of pharmacokinetics and pharmacodynamics.[10]

There is a strong demand for developing new and efficient synthetic methods as well as expanding the availability of versatile fluorine-containing synthetic building blocks and intermediates to promote medicinal chemistry, chemical biology, and molecular imaging research.[11−19] The limited availability of fluorochemicals for bioorganic and medicinal chemistry as well as pharmaceutical and agrochemical applications is mainly due to the exceptional properties and hazardous nature of fluorine and fluorochemical sources. Also, in many cases, synthetic methods developed for ordinary organic molecules do not work well for fluorochemicals because of their unique reactivity.[11−19] Therefore, the new and efficient synthetic methods applicable to organofluorine compounds, including ^{18}F radiotracers, need to be continuously developed.

This Perspective was commissioned on the occasion of my receiving the 2013 ACS Award for Creative Work in Fluorine Chemistry. Accordingly, I would like to review the research strategy and programs in my laboratory in the last three decades in perspective, which would be useful to foresee the future directions in organofluorine chemistry at the multidisciplinary interface of chemistry and biology.

1. EXPLORATION OF ORGANOFLUORINE CHEMISTRY BY MEANS OF TRANSITION-METAL CATALYSIS

My first encounter with "fluorine chemistry" was in the late 1970s, when I was a Group Leader for organometallic chemistry and homogeneous catalysis as well as organic synthesis at the Sagami Institute in Japan. At that time, the research council of the institute decided to add "fluorine chemistry" to one of its strategic research areas. To me, one of the most inspirational reports back then was the bold experiments done by Leland Clark.[20] In this paper, Clark demonstrated the capability of perfluorocarbons (PFCs) to deliver oxygen to a living mouse placed deep in a beaker filled with PFCs,[20] which clearly implied the extraordinary nature of the world of "fluorine". Of course, fluoropolymers, especially "Teflons", fluorosilicones, coolants/refrigerants, extinguishers, aerosols, etc., were the representative fluorochemicals commonly used in daily life. As for pharmaceutical drugs, only 5-FU was widely recognized followed by 9α-fluorohydrocortisone at that time.

From a strategic point of view based on synthetic organic chemistry, I reviewed and critically analyzed potential new fields of research. Then, I found that the synthetic methods by means of homogeneous catalysis were virtually nonexistent in fluorine chemistry. Accordingly, I decided to explore the interface of traditional fluorine chemistry and transition-metal-catalyzed reactions to establish a new and interdisciplinary research program in my laboratory.

We started our research program from the development of (i) unique hydrocarbonylations of fluoro-olefins that would provide versatile intermediates for the synthesis of a variety of organofluorine compounds and (ii) one-pot multistep processes exploiting the cobalt-catalyzed amidocarbonylation of aldehydes as a key unit reaction since this reaction would furnish important fundamental biochemicals, i.e., *N*-acyl α-amino acids, from an aldehyde, amide, carbon monoxide, and hydrogen. This research program proceeded smoothly, leading to successful findings of (i) the unique and remarkable effects of organofluorine substituents on the regioselectivity in the hydrocarbonylations of fluoro-olefins and the application of the highly regioselective hydroformylation to the synthesis of fluoro-amino acids, (ii) a novel ureidocarbonylation process that gives 5-(trifluoromethy1)dihydrouracils in one step, and (iii) the hydroformylation−amidocarbonylation of fluoro-olefins catalyzed by Co−Rh mixed-metal systems.

Although this program was initiated at the Sagami Institute in Japan, I moved to the State University of New York at Stony Brook in 1983 and continued the exploration and expansion of the scope of the research program.

1.1. Hydroformylation of Fluoro-olefins. Hydroformylation of alkenes is important for the practical synthesis of aldehydes,[21] and extensive studies were performed on the detailed mechanism of the reaction as well as applications to organic syntheses by the early 1980s.[22,23] Little was known, however, about the reactions of alkenes bearing perfluoroalkyl or perfluoroaryl substituents when we started our investigation.[24] It has been shown that the introduction of a trifluoromethyl or a fluoroaromatic group into organic compounds often brings about unique chemical and biological properties.[25−28] Thus, the development of new synthetic methods that can introduce these fluoro groups efficiently and selectively to the desired molecules from readily available materials had an obvious significance. In this respect, commercially available fluoro-olefins such as 3,3,3-trifluoropropene (TFP), vinyl fluoride (VF), and pentafluorostyrene (PFS) were recognized as very useful starting materials. Thus, we studied the hydroformylation of a variety of fluoro-olefins (eq 1) as one of our approaches to the functionalizations of these

$$R_fCH{=}CH_2 + CO + H_2 \xrightarrow{\text{cat.}} \underset{(n)}{R_fCH_2CH_2CHO} + \underset{(\text{iso})}{R_f(Me)CHCHO} \quad (1)$$

Rf = F, CF_3, C_2F_5, C_3F_7, C_8F_{17}, C_6F_5

building blocks by means of transition-metal catalysts. Then, we found unusually high regioselectivities and a remarkable dependency of the regioselectivities of the reaction on the catalyst metal species, which was unique in comparison with the hydroformylation of ordinary alkenes.[29−31]

1.1.1. Remarkable Dependence of Regioselectivity on the Catalyst Metal Species. The hydroformylation of TFP was carried out with $Co_2(CO)_8$, $Ru_3(CO)_{12}$, $Rh_6(CO)_{16}$, and PtCl, (DIOP)/$SnC1_2$, which are typical hydroformylation catalysts, at 100 °C and 100 atm (CO/H_2 = 1) for the Co, Pt, and Ru catalysts and at 80 °C and 110 atm (CO/H_2 = 1) for the Rh catalyst (Scheme 1).[29−31] The reaction of TFP catalyzed by $Co_2(CO)_8$ gave (trifluoromethy)propanals (TFMPAs) in 95% yield, in which a "normal" (or linear) aldehyde,

Scheme 1. Hydroformylation of TFP Catalyzed by Co, Pt, Ru, and Rh complexes

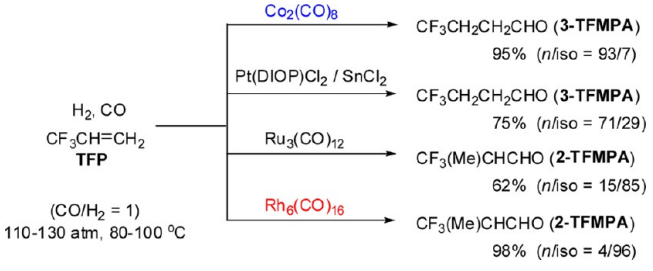

dx.doi.org/10.1021/jo400301u | J. Org. Chem. 2013, 78, 6358−6383

$CF_3CH_2CH_2CHO$ (3-TFMPA), was formed with high regioselectivity (93%). In sharp contrast with $Co_2(CO)_8$, Rh-carbonyl cluster $Rh_6(CO)_{16}$ exhibited extremely high catalytic activity and regioselectivity (96%) to give "iso" (or branched) aldehyde, $CF_3(CH_3)CHCHO$ (2-TFMPA). The Pt catalyst, $PtCl_2(DIOP)/SnCl_2$, favored the formation of normal aldehyde (n/iso =71/29), while $Ru_3(CO)_{12}$ gave isoaldehyde as the main product (n/iso =15/85). In both cases, a substantial amount of hydrogenated product, $CF_3CH_2CH_3$, was formed (25−38%). Addition of PPh_3 to the Co, Ru, and Rh catalysts considerably decreased the catalytic activities but somewhat increased the isoaldehyde selectivity. The result made a sharp contrast to the cases of ordinary olefins, where the addition of PPh_3 increased normal aldehyde se1ectivity.

Since $Rh_6(CO)_{16}$ gave excellent regioselectivity for the formation of 2-TFMPA, several other Rh catalysts were employed and their catalytic activities as well as regioselectivities examined. The results clearly indicated that the Rh(I) complexes having chlorine as a ligand, such as $RhC1(PPh_3)_3$, were less active than $HRh(CO)(PPh_3)_3$, Rh−C, $Rh_4(CO)_{12}$, and $Rh_6(CO)_{16}$, but the regioselectivity was virtually the same in all cases examined. Consequently, it was concluded that the nature of the central metal of the catalyst played a key role in determining the regioselectivity of the reaction. It was noteworthy that the metal species dependency of the regioselectivity in the this reaction was remarkable compared to that reported for propene.[22]

The reaction of PFS was carried out in a similar manner at 90 °C and 80 atm, using Co, Pt, Ru, and Rh catalysts.[29−31] Rhodium catalysts exhibited high catalytic activity to give isoaldehyde, $C_6F_5(CH_3)CHCHO$ (2-PFPPA), with excellent regioselectivity (97−98%) in quantitative yields, while $Co_2(CO)_8$ gave normal aldehyde (3-PFPPA) as the major product, with regioselectivity (79−90%) not as high as that observed in the reaction of TFP. The Ru catalyst, $Ru_3(CO)_{12}$, showed rather low catalytic activity (49% conversion), giving isoaldehyde as the major isomer (22% yield, b/n = 74/26), accompanied by a substantial amount of hydrogenated product, $C_6F_5CH_2CH_3$ (25%). The Pt catalyst, $PtCl_2(DIOP)/SnCl_2$, showed a high catalytic activity (100% conversion in 4 h, 76% aldehyde yield), but virtually no regioselectivity was observed and the hydrogenation of PFS took place as a severe side reaction (20%). Thus, the dependency of regioselectivity on the metal species was similar to that for TFP, and the observed regioselectivity was also remarkably high compared with that reported for styrene.[32−34]

A kinetic study was performed for the $Rh_4(CO)_{12}$- and $Co_2(CO)_8$-catalyzed reactions of PFS.[30] At 100 °C and 82 atm (CO/H_2 = 1) with 1.0×10^{-5} M catalyst concentration, the Rh-catalyzed reaction was first order in PFS concentration, and the apparent rate constant was calculated to be 6.2×10^4 s^{-1}; i.e., the turnover number was estimated to be 55800 h^{-1} per Rh metal. The Co-catalyzed reaction with 1.0×10^{-2} M catalyst concentration at 100 °C and 82 atm (CO/H_2 = 1) was also first order in PFS concentration, and the apparent rate constant was calculated to be 1.6×10^{-5} s^{-1}; i.e., the turnover number per cobalt metal was 2.88 h^{-1}. Thus, the Rh catalyst was ca. 20000 times more active than the Co catalyst per metal provided that all metal species participate in the catalysis.

On the basis of the fact that the addition or the introduction of tertiary phosphines to the catalyst caused only a slight change in regioselectivity, in sharp contrast to the hydroformylation of propene or styrene using the same catalysts, both TFP and PFS should have a large binding constant with catalyst metal species, and thus, these fluoro-olefins should act as important ligands that stabilize the catalysts during the reaction.[30]

In order to examine the effects of perfluoroalkyl substituents longer than the trifluoromethyl group on the regioselectivity, the reactions of other fluoro-olefins of the type $R_fCH{=}CH_2$ catalyzed by $Rh_4(CO)_{12}$ were carried out, wherein R_f were C_2F_5 (PFB), C_3F_7 (HPFP), and C_8F_{17} (HPDFD) (eq 2).[30] The

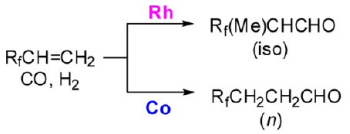

(2)

Rf = C_2F_5, C_3F_7, C_8F_{17}, C_6F_5

reactions gave the corresponding branched aldehydes with lower regioselectivity (72−83%) than that for TFP under the standard conditions, i.e., at 80 °C and 100 atm (CO/H_2 = 1). Nevertheless, higher selectivity (91−97%) was achieved when the reactions were carried out at 60 °C.

The reaction of vinyl fluoride (VF) catalyzed by Rh, Ru, and Co complexes was also carried out (eq 3), which gave 3-fluoropropanal (2-FPA) exclusively regardless of the catalyst species used.[30]

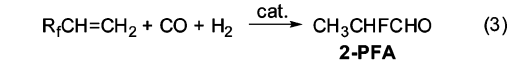

(3)

cat. = $Rh_4(CO)_{12}$, $HRh(CO)(PPh_3)_3$, $Ru_3(CO)_{12}$, $Co_2(CO)_8$

Mechanism of the Highly Regioselective Hydroformylation. The observed marked dependence of regioselectivity on the catalyst species was accommodated by taking into account the stability of isoalkyl−[M] species, the capability of isoalkyl−[M] species for isomerization, and the relative rate of the migratory insertion of CO into isoalkyl−[M] and n-alkyl−[M] bonds.[29,30] As shown in Scheme 2, when a substituent bearing a strong "group electronegativity" is introduced into an olefin, the metal−Cα bond of a π-olefin−[M] complex (**IA**) should be stronger than the metal−Cβ bond because of substantial

Scheme 2. Mechanism of Highly Regioselective Hydroformylation of Fluoro-olefins

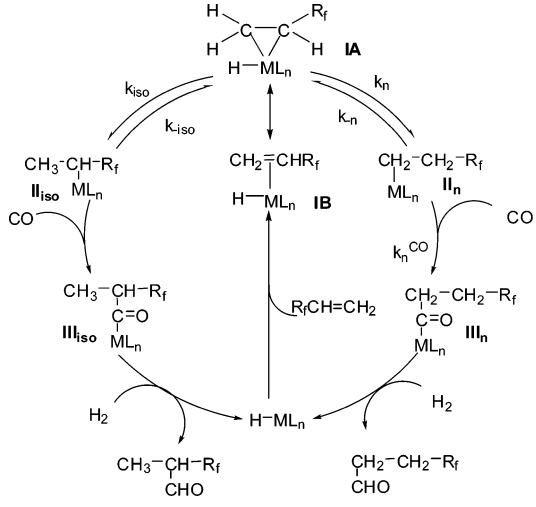

dx.doi.org/10.1021/jo400301u | J. Org. Chem. 2013, 78, 6358−6383

stabilization of the formal negative charge developing on Cα. Thus, the formation of isoalkyl−[M] species ($\mathbf{II_{iso}}$) should be much more favorable than that of *n*-alkyl−[M] species ($\mathbf{II_n}$) *regardless of the group VIII transition-metal species.* In fact, the results of the reactions of vinyl fluoride (VF) provide strong supporting evidence for this hypothesis.

The iso/*n* ratio of aldehydes should reflect the ratio of the intermediate iso- and *n*-acyl−[M] species ($\mathbf{III_{iso}}$ and $\mathbf{III_n}$) (Scheme 2) under sufficient pressure of hydrogen. Thus, it is deduced that in the Rh-catalyzed reaction, $k_{iso} \gg k_{-i}$ and $k_n^{CO} \gg k_{-n}$, and thus the initially formed isoalkyl−[Rh] species ($\mathbf{II_{iso}}$, M = Rh) generates the isoacyl-[Rh] species ($\mathbf{III_{iso}}$, M = Rh) and gives the isoaldehyde with high regioselectivity. In sharp contrast, the rate constants in the Co-catalyzed reaction are $k_{-n} \gg k_n^{CO}$ and $k_{-i} \gg k_{iso}^{CO}$; $k_n^{CO} > k_{iso}^{CO}$. This is because the CO insertion to $\mathbf{II_n}$ (M = Co) is sterically less demanding than that to $\mathbf{II_{iso}}$ (M = Co). Accordingly, the alkyl−[M] intermediates, $\mathbf{II_{iso}}$ and $\mathbf{II_n}$ (M = Co), should be in a pre-equilibrium, and then the reaction gives the normal aldehyde selectively. The Rh- and Co-catalyzed reactions are extremely selective cases, and the Pt- and Ru-catalyzed reactions are in between the two extreme cases.

In addition to these kinetic aspects, we should take into account the fundamental difference between each isoalkyl−[M] intermediate, i.e., the size of the metal and the polarizability of the metal−carbon bond. Thus, the relative stability of $\mathbf{II_{iso}}$ can be estimated to increase in the order Rf(Me)CH-**Co**L_n < Rf(Me)CH-**Pt**L_n < Rf(Me)CH**Ru**L_n < Rf(Me)CH-**Rh**L_n.[30]

It is worth noting that these mechanistic details were revealed because of the use of fluoro-olefins as unique substrates for the hydroformylation reaction. In this case, organometallic chemistry and catalysis research greatly benefited from fluorine compounds. In turn, fluorine chemistry also benefited from the discovery of highly regioselective hydroformylation processes, which provided versatile fluorine-containing aldehydes. In fact, immediately after the discovery of highly regioselective hydroformylation of TFP by Rh-catalyzed process, I envisioned that we should be able to produce a series of "CF_3-chemicals" from TFMAs.[35]

1.2. Hydroesterification and Hydrocarboxylation of Fluoro-olefins. Hydrocarbonylations of olefins serves as a convenient method for the synthesis of the corresponding esters or carboxylic acids.[22,36] Despite extensive mechanistic studies as well as applications of the reactions to organic syntheses, little attention had been paid to the reactions of fluoro-olefins before we started the investigation on this subject.

The screening of typical transition-metal complexes in the hydrocarbonylations of TFP and PFS revealed that only Pd complexes with phosphine ligands showed sufficient catalytic activity to promote the reaction under the given reaction conditions.[37] As Scheme 3 shows, the Pd-complex-catalyzed hydroesterification of TFP and PFS gave branched esters, R_f(Me)CHCOOR, in good to excellent regioselectivity, while the corresponding hydrocarboxylation afforded linear acids, $R_fCH_2CH_2COOH$, in excellent yield and regioselectivity. Plausible mechanisms were proposed to accommodate the observed marked difference in regioselectivity for these two reactions.

Scheme 3. Pd-Catalyzed Hydroesterification and Hydrocarboxylation of TFP and PFS

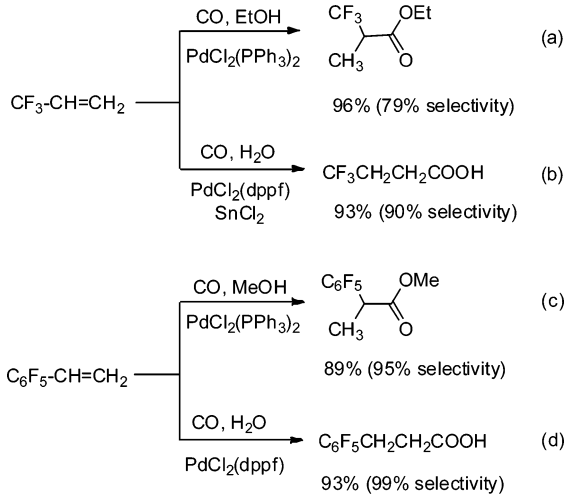

2. SYNTHESIS OF FLUORO ANALOGUES OF ALIPHATIC AND AROMATIC α-AMINO ACIDS

By the mid 1980s, it was shown that fluorinated analogues of naturally occurring biologically active compounds often exhibited unique physiological activities.[25,28,38] For example, fluorinated pyrimidines acted as anticancer/antiviral agents, and some fluoro-aromatic compounds as well as CF_3-aromatic compounds were used as nonsteroidal anti-inflammatory drugs, antifungal agents, human antiparasitic agents, central nervous system agents for psycho-pharmacology, diuretics agents, and antihypertensive agents. Some fluoro-amino acids acted as "suicide substrate enzyme inactivators", showing strong antibacterial activities and some of them also acted as antihypertensive agents.[28] In the mid to late 1980s, there was an increasing interest in the incorporation of fluoro-amino acids into peptides.[39−43] Accordingly, it was timely and important to develop new and efficient methods for the synthesis of fluoro-amino acids at that time (and even now in the 2010s!).

We found that the fluoro-aldehydes obtained in the hydroformylation of TFP and PFS, described above, served as excellent intermediates for the synthesis of fluoro-amino acids. Thus, we developed efficient synthetic routes to 4,4,4-trifluorovaline (TFV), 5,5,5-trifluoronorvaline (TFNV), 5,5,5-trifluoroleucine (TFL), 6,6,6-trifluoronorleucine (TFNL), 4,5,6,7-tetrafluorotryptophan (tryptophan-f_4), and related compounds from the fluoro-aldehydes by means of transition-metal-catalyzed transformations as well as enzymatic reactions.[44]

2.1. 4,4,4-Trifluorovaline (TFV) and 5,5,5-Trifluoronorvaline (TFNV). TFV and TFNV were synthesized using Co-catalyzed amidocarbonylation of 2-TFMPA and 3-TFMPA, respectively. The amidocarbonylation of 2-TFMPA and 3-TFMPA with acetamide catalyzed by $Co_2(CO)_8$ (CO/H_2 (1/1) 100 atm, 120 °C) gave Ac-TFV and *N*-Ac-TFNV, respectively, in good yields, which were further hydrolyzed to the corresponding free amino acids (eqs 4 and 5).[44]

We also successfully carried out the kinetic optical resolution of Ac-TFNV, using porcine kidney acylase I (25 °C, pH 7.0) to give (*S*)-TFNV and (*R*)-Ac-TFNV with high enantiopurities, which were readily separated (eq 6).[44] (*R*)-Ac-TFNV was further hydrolyzed to (*R*)-TFNV with 3 M HCl. The enantiopurities of (*S*)-TFNV and (*R*)-TFNV were determined by Mosher's MTPA method[45] (^{1}H and ^{19}F NMR).

dx.doi.org/10.1021/jo400301u | J. Org. Chem. 2013, 78, 6358−6383

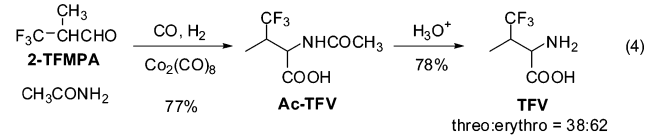

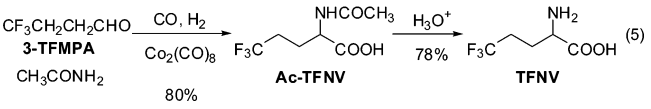

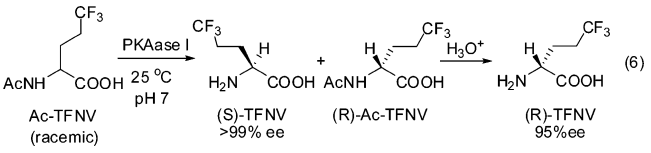

It has been shown that TFNV inhibits the growth of *E. coli* and may be used as a growth regulatory factor in microbiology.[46] TFV serves as a modifier of biologically active peptides in protein engineering and chemical biology. In fact, both TFNV and TFV are commercially available from more than several vendors now, and indeed, (2*S*)-TFV has been extensively used in protein design and chemical biology, as we envisioned in late 1980s.[47]

2.2. 5,5,5-Trifluoroleucine (TFL) and 6,6,6-Trifluoronorleucine (TFNL). TFL and TFNL were synthesized via azlactones prepared from 2-TFMPA and 3-TFMPA, respectively (Scheme 4, (a) and (b)).[44] The azlactones were subjected to alcoholysis to give the corresponding dehydroamino acid esters **3** and **4**. (*Z*)-Dehydroamino acid **3c** was obtained by hydrolysis of **1**-*Z*. Then, the (*Z*)-dehydroamino acid and esters (**3**-*Z* and **4**-*Z*) were hydrogenated over Pd/C followed by hydrolysis to give the corresponding amino acids TFL and TFNL. The azlactones (**1**-*Z* and **2**-*Z*) were also treated with hydriodic acid/red phosphorus to give TFL and TFNL directly.

It is worthy of note that the chiral 2,2,2-trifluoroisopropyl group acted as an effective stereogenic center in the hydrogenation of **3**-*Z* over Pd/C, yielding Bz-TFL-OR (Scheme 4, (a)).[44] Thus, the hydrogenation of **3a**-*Z*, **3b**-*Z*, and **3c**-*Z* in THF at ambient temperature and pressure of H_2 gave Bz-TFL-OMe (85:15 dr), Bz-TFL-OEt (90:10 dr), and Bz-TFL−OH (82:18 dr), respectively, in quantitative yield. It was rather surprising that the "chiral isopropyl group" was able to induce a high degree of stereoselectivity. It was strongly suggested that the trifluoromethyl group was not only a bulkier substituent than methyl but also imposed a unique electronic effect on the Pd−metal surface.

Optically active (*S*)-*N*-Bz-TFNL-OMe (87−89% ee) was obtained quantitatively by asymmetric hydrogenation of **4a**-*Z* (R = Me) using a cationic Rh catalyst with diPAMP[48] at 40 °C and 1 atm of H_2 in ethanol.[44] (*S*)- and (*R*)-TFNL with excellent enantiopurities (>98% ee) were obtained through enzymatic resolution of racemic Ac-TFNL using porcine kidney acylase I in a manner similar to that for Ac-TFNV (eq 7).[44]

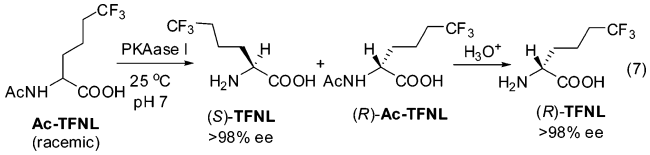

We envisioned that TFL and TFNL would serves as unique modifiers of biologically active peptides in protein engineering and chemical biology. As we anticipated in the late 1980s, both TFL and TFNL are commercially available from more than several vendors now, and indeed, (2*S*)-TFL has been extensively used in protein design and chemical biology.[47]

2.3. 4,5,6,7-Tetrafluorotryptophan and Related Compounds. As the importance of biologically active compounds bearing the indole skeleton such as tryptophan, tryptamine, indoleacetic acid, and alkaloids was well recognized, tetrafluoro analogues of indoles were synthesized from 2-PFPPA.[44,49] The reaction of 2-PFPPA with allylamine followed by cyclization using lithium diisopropylamide (LDA) as a base and deprotection of the indole nitrogen gave 3-Me-indole-f_4 in 72% from 2-PFPPA (eq 8).

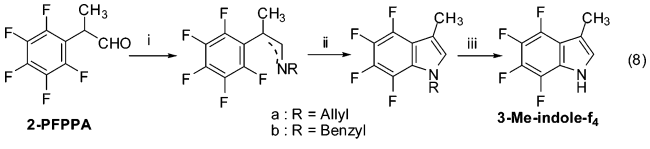

i) RNH_2, $MgSO_4$; ii) LDA, -78 °C; iii) $RhCl_3 3H_2O$, (b) H_3O^+

The SeO_2 oxidation of *N*-Ac-3-Me-indole-f_4 **5** gave indole-f_4-3-CHO in 86% yield (eq 9). The SeO_2 oxidation of **5** in the

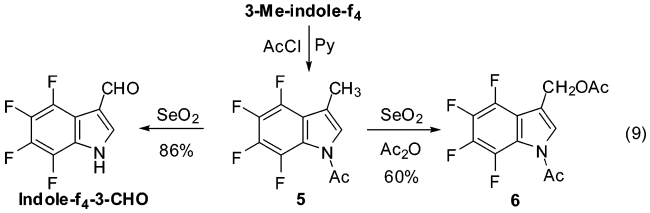

Scheme 4. Synthesis of Trifluoroleucine and Trifluoronorleucine from 2-TFMPA and 3-TFMPA via Azlactones

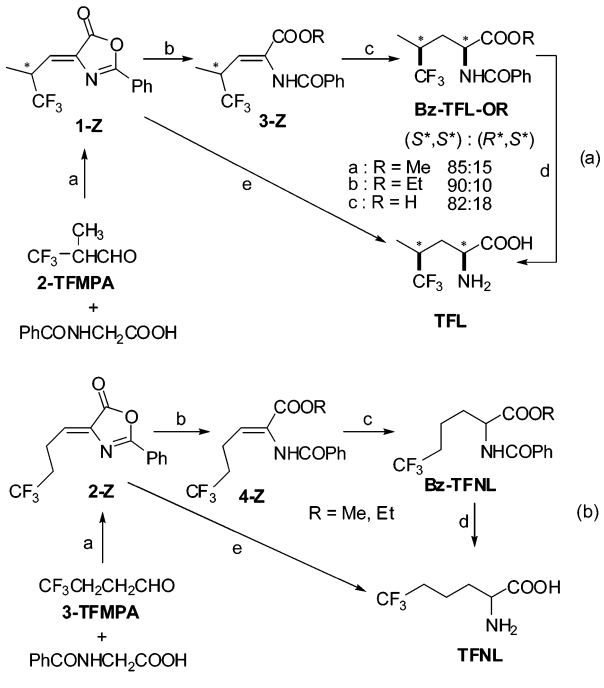

a) Ac_2O/THF/$Pb(OAc)_2$; b) ROH/base; c) H_2/Pd-C, THF, ambient; d) H_3O^+; e) HI/P.

dx.doi.org/10.1021/jo400301u | J. Org. Chem. 2013, 78, 6358−6383

presence of acetic anhydride gave 1-Ac-3-(AcO-methyl)indole-f_4 **6** in 60% yield (eq 9). 3-(AcO-methyl)indole-f_4 **6** and indole-f_4-3-CHO were very useful intermediates for the synthesis of tetrafluoro analogues of tryptophan, tryptamine, and indoleacetic acid.[44]

Thus, tryptamine-f_4 was synthesized from indole-f_4-3-CHO in 83% overall yield through condensation with nitromethane, followed by $LiAlH_4$ reduction, while tryptophan-f_4 was obtained in four steps in 51% overall yield through Erlenmeyer's azlactone method (eq 10). The reaction of **6** with piperidine

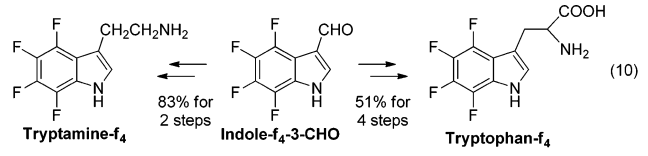

(10)

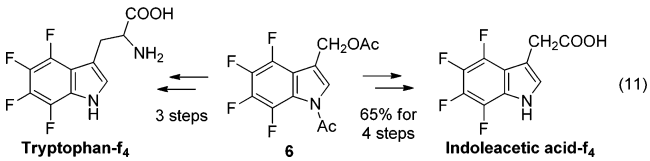

(11)

gave 3-(piperidinomethyl)indole-f_4 in 97% yield, which was a known key intermediate for tryptophan-f_4 in 2 steps (eq 11). Also, indoleacetic acid-f_4 was synthesized from **6** in four steps via 3-(cyanomethyl)indole-f_4 (eq 11).

Since it was shown that tryptophan-f_4 strongly inhibits both the tryptophanyl hydroxamate and aminoacyl *t*-RNA formation,[50,51] the tetrafluoro analogues of tryptamine, indoleacetic acid, and other indole derivatives were expected to possess unique physiological activities. Tryptophan-f_4 has been used in enzymology, protein engineering and chemical biology.[52,53]

3. CARBONYLATIONS OF α-(TRIFLUOROMETHYL)VINYL BROMIDE

3.1. Synthesis of 2-Trifluoromethylacrylic Acid through Pd-Catalyzed Carboxylation. The bromination of TFP promoted by photoirradiation followed by dehydrobromination on KOH gave 2-Br-TFP in high yield.[54] The carboxylation of 2-Br-TFP catalyzed by a Pd catalyst, e.g., $PdCl_2(PPh_3)_2$ or $PdCl_2$(dppf), in the presence of Et_3N in DMF or THF afforded 2-(trifluoromethyl)acylic acid (2-TFMAA) in 65−78% yield (eq 12).[55]

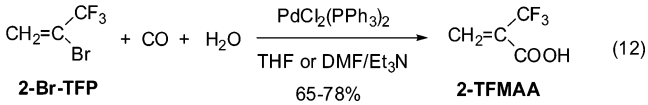

(12)

A variety of trifluoromethacrylates, $CH_2{=}C(CF_3)COOR$, were readily prepared from 2-TFMAA, which were potentially very useful monomers for fluorine-containing polymethacrylates (Figure 1). Copolymerizations with other olefins, e.g., methyl methacrylate (MMA) and styrenes, were also possible. In fact, the homo- and copolymerizations of methyl trifluoromethacrylate (MTFMA) were reported[56] with regard to the development of new radiation-sensitive polymers for resists in microelectronic fabrication processes, wherein MTFMA was prepared from trifluoroacetone. Copolymers of TFMA esters with styrene and substituted styrenes were also prepared.[57] We synthesized a variety of new trifluoromethacrylates bearing polyfluoroalkyl ester moieties,[58,59] which would serve as monomers for potential photoresists and as a

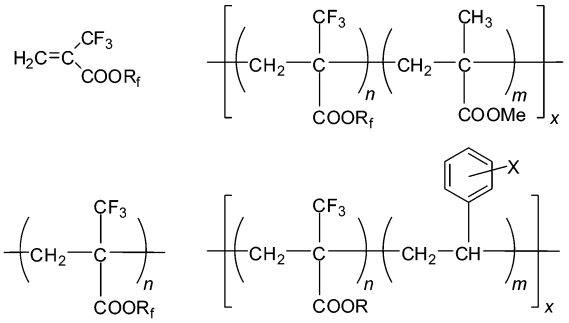

Figure 1. Homo- and block copolymers of 2-TFMAA esters.

component of optical fibers. Although we did not follow up this line of research in my laboratory, TFMA esters have been extensively studied and are still under active investigation for the development of photoresists for lithography using short wavelength light, e.g., 157/193 nm,[60−62] as we envisioned in the 1980s.[24,58]

3.2. α-Trifluoromethyl-β-alanine (α-TFM-β-Ala). We found that the addition of gaseous ammonia to 2-TFMAA at 0−5 °C in CH_2Cl_2 gave a novel β-amino acid, α-trifluoromethyl-β-alanine (α-TFM-β-Ala), in excellent yield.[44] However, the reaction sometimes gave double and triple Michael addition products, depending on the reaction conditions. The use of hexamethyldisilazane (HMDS) in an attempt to protect the C-terminus of TFMAA with a TMS group resulted in an addition of H_2NTMS, generated in situ, to *O*-TMS-TFMAA, giving *N,O*-bis-TMS-α-TFM-β-Ala (**7**) in quantitative yield. No trace of *N,N,O*-tris-TMS-α-TFM-β-Ala was detected. Also, Michael addition of HMDS to the methyl and benzyl esters of TFMAA did not proceed at all. The disilylated α-TFM-β-Ala (**7**), thus obtained, was treated with MeOH to give α-TFM-β-Ala in nearly quantitative yield (eq 13).[44]

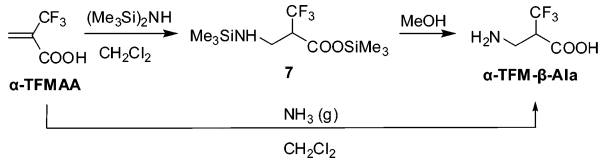

(13)

α-TFM-β-Ala did not exhibit any antibacterial activity in our preliminary screening. However, an enkephalin analogue bearing α-TFM-β-Ala, Tyr-D-Ala-(α-TFM-β-Ala)-Phe-Met, has shown fairly strong analgesic effects.[63,64] This suggested that the novel fluoro-β-amino acid would serve as a modifier for a variety of peptide hormones and other physiologically active peptides, although a method to obtain enantiopure material was needed. It should be noted that α-TFM-β-Ala is now commercially available from more than several vendors.

3.3. "Ureidocarbonylatlon" of 2-Bromotrifluoropropene (2-Br-TFP) Catalyzed by a Pd−Phosphine Complex. The Pd-complex-catalyzed amidation of vinyl halides was shown to be a convenient method for the synthesis of α,β-unsaturated amides.[65] However, nothing was known for the Pd-catalyzed reaction of vinyl halides with ureas instead of amines. Accordingly, we investigated the Pd-catalyzed carbonylation reaction of 2-Br-TFP with a urea. Our hypothesis was that both nitrogen termini of a urea would possess sufficient nucleophilicity so that the reaction should give the dihydrouracil skeleton

dx.doi.org/10.1021/jo400301u | J. Org. Chem. 2013, 78, 6358−6383

in one step. Actually, the reaction proceeded as anticipated to give 5-CF_3-5,6-dihydrouracil **8** in good yield, and this novel carbonylation process was termed "ureidocarbonylation". A general scheme for this novel process is shown in eq 14.[66]

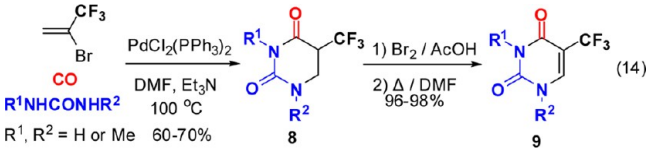

However, when unsubstituted urea was employed, the yield of **8d** (R^1 = R^2 = H) was low. 5-CF_3-dihydrouracils **8**, thus obtained, were readily converted to the corresponding 5-CF_3-uracils **16** by treating with bromine[67] in nearly quantitative yields (eq 9).[66] It should be noted that **8** exhibited substantial antitumor activity against ascitic mastocarcinoma MM2 cells.[55] A proposed mechanism for the "ureidocarbonylation" is illustrated in Scheme 5.[66]

Scheme 5. Mechanism of Pd-Catalyzed Ureidocarbonylation of 2-Br-TFP

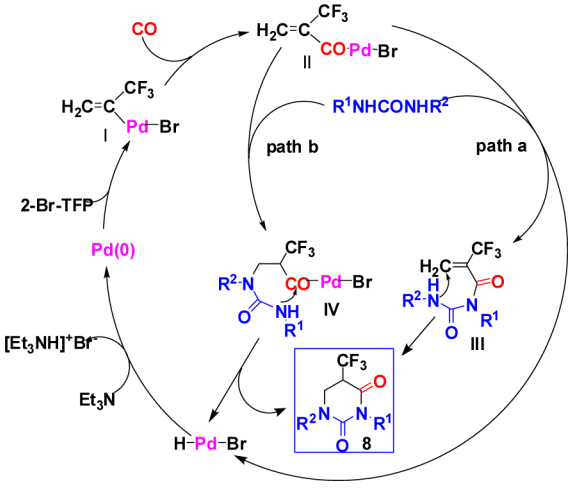

We also found a simple method for the synthesis of **8** as well as its thio analogues just by heating a mixture of 2-TFMAA and a urea or thiourea in the presence of acetic anhydride at 80–100 °C, which afforded the corresponding **8** or its thio analogues in 50–84% yield (eq 15).[55,68] Most importantly, 5-CF_3-5,6-dihydrouracil (**8d**) was obtained in 67% yield (unoptimized) using this method, which was converted to 5-CF_3-uracil (**9d**) in excellent yield.[55,68]

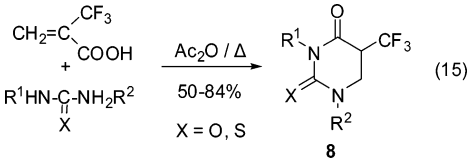

It is worthy of note that the processes for producing 2-TFMAA from 2-Br-TFP as well as **9d** from 2-TFMAA and urea followed by dehydrogenation were developed as commercial processes by Japan Halon (now Tosoh F-Tech). Furthermore, **9d** was successfully applied to the commercial synthesis of trifluridine (trifluorothymidine), an antiherpes antiviral drug,[69] primarily used on the eye topically, such as "Viroptic". This commercial process was developed by Japan Halon and Tokyo Yuki Gosei Kogyo in Japan in the early 1990s and is still operating at present.

4. HYDROFORMYLATION–AMIDOCARBONYLATION OF FLUORO-OLEFINS: HIGHLY REGIOSELECTIVE DIRECT SYNTHESIS OF FLUOROAMINO ACIDS FROM FLUORO-OLEFINS

4.1. Hydroformylation–Amidocarbonylation of Trifluoropropene (TFP). The hydroformylation–amidocarbonylation (HF-AC) of TFP was investigated since the reaction should give the corresponding normal or iso *N*-acetylamino acid, Ac-TFNV or Ac-TFV, directly from TFP if the extremely regioselective hydroformylation was successfully combined with amidocarbonylation. As Scheme 6 shows, the Co-catalyzed

Scheme 6. Hydroformylation–Amidocarbonylation of TFP

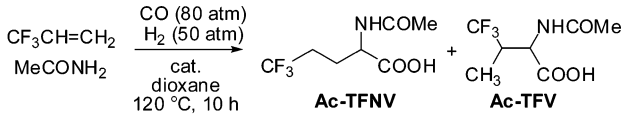

Catalyst	Yield (%)			
$Co_2(CO)_8$	83	96	:	4
$Co_2(CO)_8$-$Rh_6(CO)_{16}$	87	6	:	94

reaction gave Ac-TFNV with 96% selectivity, while the reaction catalyzed by the Rh–Co binary system ($Co_2(CO)_8$/$Rh_6(CO)_{16}$ = 50) under the same conditions gave Ac-TFV with 94% selectivity.[70] The latter result clearly indicated that the Rh-catalyzed hydroformylation took place exclusively in the first step to give 2-TFMPA with high selectively, which was effectively incorporated into the subsequent Co-catalyzed amidocarbonylation.

4.2. Hydroformylation–Amidocarbonylation of Pentafluorostyrene (PFS). In contrast to the results obtained for the reactions of TFP, the attempted regioselective HF-AC of PFS catalyzed by the Co–Rh binary catalyst system as well as $Co_2(CO)_8$ under similar conditions gave unexpected results. The detailed study of the reaction revealed interesting mechanistic aspects of Co–Rh mixed-metal catalyst systems, including a novel $CoRh(CO)_7$-catalyzed process.[70]

The HF-AC of PFS with acetamide catalyzed by $Co_2(CO)_8$ gave *N*-Ac-4-C_6F_5-homoalanine (**10**) with 90–92% regioselectivity (Scheme 7). This regioselectivity was much higher than that (79%) of the simple hydroformylation in benzene.[30] The reaction catalyzed by $Co_2(CO)_8$/$Rh_6(CO)_{16}$ gave *N*-acetyl-3-C_6F_5-homoalanine (**11**) with only ca. 80% regioselectivity, which was much lower than the excellent regioselectivity (98%)

Scheme 7. Hydroformylation–Amidocarbonylation of PFS

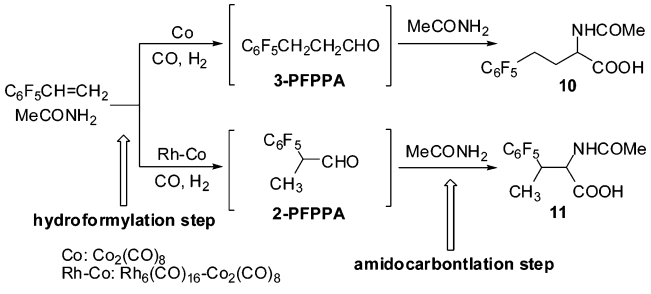

dx.doi.org/10.1021/jo400301u | J. Org. Chem. 2013, 78, 6358–6383

of the simple hydroformylation in benzene.[30] To accommodate these unexpected results, a detailed mechanistic study was performed to clarify these anomalies.[70]

It was found that the hydroformylation was the rate- and regioselectivity-determining step and the presence of acetamide substantially increased the normal selectivity, probably by forming an active species $HCo(CO)_n(CH_3CONH_2)_m$. This catalyst species, however, substantially increased the formation of hydrogenation product, C_6F_5Et. If the Co and Rh catalysts worked independently, the ratio of normal aldehyde formation should increase at higher Co/Rh ratios and eventually the normal aldehyde should become the major product. However, contrary to this assumption, an interesting leveling phenomenon of regioselectivity was observed, i.e., the iso/*n* ratio decreases from 94/6 at Co/Rh = 5 to 88/12 at Co/Rh = 25, but the ratio was unchanged (87/13) even at a Co/Rh ratio of 100! This leveling phenomenon was best interpreted by taking into account the formation of and the catalysis by a Co−Rh mixed-metal complex. When we reached this conclusion, Horváth, Bor, and Pino at ETH reported synthesis, characterization, and some reactions of an interesting coordinatively unsaturated Co−Rh mixed metal complex, $CoRh(CO)_7$ (eq 16),[71−73] which was eventually identified as the catalyst species in our HF-ADS reaction.

$$Rh_4(CO)_{12} + 2Co_2(CO)_8 \overset{K_1}{\rightleftharpoons} 4CoRh(CO)_7 \qquad (16)$$

In order to directly confirm the catalyst species in dioxane, we performed a high pressure FT-IR study on the Co−Rh mixed metal complex system, which provided strong supporting evidence for the $CoRh(CO)_7$ catalysis.

Next, the relative activities of catalyst species were evaluated on the basis of the equilibrium constant K_1 reported for eq 14.[73] The iso/*n* ratio vs Co/Rh ratios were calculated and plotted with several given relative catalytic activities. In dioxane, the relative catalytic activity of 54/mol (9/Rh) for $Rh_6(CO)_{16}$/$CoRh(CO)_7$ showed a very good agreement with the experimental results. The relative catalytic activity for $Rh_6(CO)_{16}/Co_2(CO)_8$ was calculated to be ca. 400000, i.e., 133000 per metal. Finally, kinetic studies were performed to compare the results with those predicted by calculations based on the regioselectivity. The kinetic measurements in dioxane provided the relative activity values as follows: $Rh_6(CO)_{16}$/$CoRh(CO)_7$ = 3.8/Rh, $Rh_6(CO)_{16}/Co_2(CO)_8$ = 398000. Consequently, the results of these two independent evaluation methods were in very good agreement in spite of various assumptions and simplification for calculations.[70]

Overall, this study provided a rare and successful example of the elucidation of mixed-metal catalysis, in which actual active catalyst species and their direct precursors were detected spectroscopically and the observation corresponded almost perfectly to the mechanism proposed based on the regioselectivity analysis. It should be emphasized that the discovery of $CoRh(CO)_7$ catalysis as well as the successful mechanistic studies in organometallic chemistry and catalysis were only possible by the use of unique fluoro-olefin, PFS.

From the synthetic viewpoint, a highly regioselective formation of fluoro-amino acid **12**, directly from PFS is noteworthy. The reaction of PFS using a $Co_2(CO)_8$ (5.0 mol %)−$Rh_4(CO)_{12}$ (0.05 mol %) catalyst system gave **12** in 80% yield and 98.2% regioselectivity at 60 °C for 6 h and then 125 °C for 5 h under 75 atm of CO and 48 atm of H_2.[70] Base-promoted cyclization of **12** gave *N*-Ac-2-hydroxycarbonyl-3-methyl-2,3-dihydro-4,5,6,7-tetrafluoroindole (**13**) in 92% yield, which could be converted to a variety of fluoro-indoles and fluoro-alkaloids (Scheme 8).[70]

Scheme 8. Tetrafluoroindole Synthesis from PFS via Highly Regioselective Hydroformylation−Amidocarbonylation

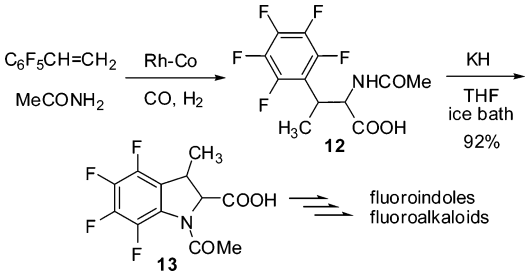

5. APPLICATIONS OF TRIFLUOROMETHYL-CONTAINING AMINO ACIDS TO ENZYME INHIBITORS

5.1. Trifluoromethyl Analogues of Captopril as Inhibitors of Angiotensin-Converting Enzyme. It has been shown that inhibitors of angiotensin converting enzyme (ACE) play key roles in the control of blood pressure as therapeutic agents. Since the development of potent ACE inhibitors captopril[74,75] and enalaprilat,[76] various analogues of these drugs have been designed and synthesized, and their ACE inhibitory activity has been examined. However, little attention had been paid to the synthesis and activity of fluorinated analogues until we started our investigation in the late 1980s.[77] Thus, we designed and synthesized CF_3 analogues of captopril and evaluated their ACE inhibitory activity to examine the effect of fluorine incorporation on the potency.

Chiral Michael acceptor 2-CF_3-acryloyl-(*S*)-Pro-OBu-*t* (**14**) was prepared through the facile coupling of (*S*)-Pro-OBu-*t* and α-CF_3-acryloyl chloride,[55] derived from 2-TMFAA in 85% yield (Scheme 9).[78]

Conjugate addition of thiolacetic acid to **14** gave a diastereomeric mixture of adducts, (*R*,*S*)-**15** and (*S*,*S*)-**15** (*RS*/*SS* = 1/2) in 70% yield, which were separated by MPLC (Scheme 9).[78,79] The stereochemical assignments were

Scheme 9. Synthesis of (*R*,*S*)- and (*S*,*S*)-Captopril-f_3

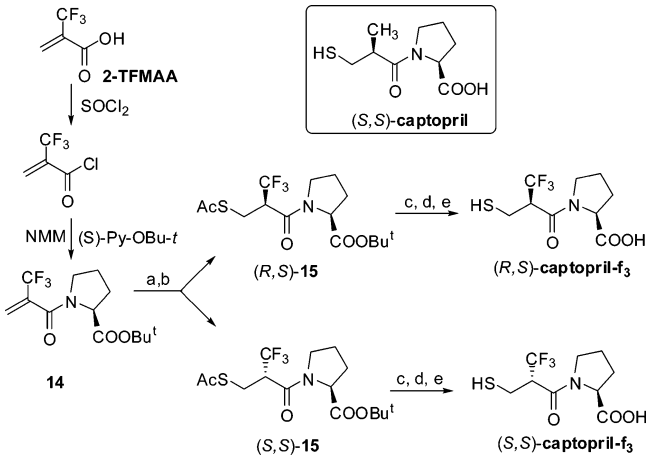

(a). AcSH, THF, r.t., 20h; (b). MPLC separation, ***RS*/*SS*** = 1/2, 70% total (2 steps); (c) Me_3SiI, $CHCl_3$, r.t. 85-92%; (d). MeOH-NH_3, r.t.; (e). $NaBH_4$, 2-propanol, 78-82% (2 steps).

dx.doi.org/10.1021/jo400301u | J. Org. Chem. 2013, 78, 6358−6383

unambiguously made on the basis of the X-ray crystal structure of (*S*,*S*)-**15**. Syntheses of (*R*,*S*)-captopril-f_3 and (*S*,*S*)-captopril-f_3 are illustrated in Scheme 9.[78,79]

The CF_3-analogues of captopril were subjected to in vitro enzyme inhibitory assay against ACE based on the method of Holmquist et al. using the tripeptide, [3-(2-furyl)acryloyl)]-Phe-Gly-Gly, as the substrate.[80] The results are listed in Table 1.[78,79] (*S*,*S*)-Captopril was also used as the reference in this assay.

Table 1. ACE Inhibitory Activity of CF_3-Analogues of Captopril

ACE inhibitor	IC_{50} (M)
(*R*,*S*)-captopril-f_3	2.9×10^{-10}
(*S*,*S*)-captopril-f_3	4.8×10^{-7}
(*S*,*S*)-captopril	3.6×10^{-9}

As Table 1 shows, (*R*,*S*)-captopril-f_3 was found to be extremely potent (IC_{50} 10^{-10} M level), while the corresponding diastereomer, (*S*,*S*)-captopril-f_3, was much less potent by 3 orders of magnitude. A similar difference in potency was reported for (*S*,*S*)- and (*R*,*S*)-captopril, i.e., the (*S*,*S*)-isomer was more potent than the (*R*,*S*)-isomer by a factor of 100.[74] It is worthy of note that (*R*,*S*)-captopril-f_3 is at least 1 order of magnitude more potent than (*S*,*S*)-captopril.

The considerably higher potency of (*R*,*S*)-captopril-f_3 than (*S*,*S*)-captopril may be ascribed to the hydrophobicity and the stereoelectronic effects of the CF_3 group. Namely, the incorporation of the (2*R*)-CF_3 group may significantly contribute to an increase in attractive interaction with the hydrophobic binding site of ACE. Also, the stereospecific incorporation of (2*R*)-CF_3 may cause strong restriction of rotation around the amide bond because of the stereoelectronic effect of the CF_3 group. This would fix the inhibitor in the favorable conformation such that strong binding with the active site is achieved without sacrificing energy for conformational change.

In fact, the energy minima for hypothetical binding conformations based on molecular mechanics calculations of (*S*,*S*)-captopril and (*R*,*S*)-captopril-f_3 indicated the latter compound to be more favorable by 1.3 kcal/mol, which corresponds to 10-fold difference in activity.[78,79] Also, the 8.33 kcal/mol difference between (*R*,*S*)-captopril-f_3 and (*S*,*S*)-captopril-f_3 calculated corresponds to the 1,700 times difference in the activity. In addition, a semiempirical approach was employed to further examine the inhibitor-enzyme interaction by using the *n*-SCF-molecular mechanics program (PIMM).[81] This calculation indicated that the binding energy of (*R*,*S*)-captopril-f_3 was 2.4 kcal/mol more favorable than (*S*,*S*)-captopril.[87]

5.2. Potent Enkephalin Analogues with Trifluoromethyl-Containing Amino Acid Residues. Enkephalins, "opioid peptides" in the brain, are known to play important roles as analgesics, regulators of blood pressure, and neurotransmitters. In the hope of developing nontoxic, nonaddictive, and effective analgesics, replacing morphine, structural modifications of enkephalins have been extensively studied, and a variety of analogues have been developed.[82] Neurobiological studies have revealed the presence of the major opiate receptors μ, δ, and κ that mediate the analgesic effects of opiates and opioid peptides including enkephalins.[83] Thus, the discovery and development of opiate receptor specific ligands has been of active interest in medicinal chemistry as well as neurobiology. However, in spite of extensive studies on enkephalin analogues, little attention had been paid to the fluoro-analogues of enkephalins[84] when we started our investigation in the early 1990s.

The major nemesis of these opioid peptides is a group of degrading enzymes that cleave the peptide into inactive fragments.[85,86] These enzymes include (i) aminopeptidase M and membrane-bound aminopeptidase(s), cleaving enkephalins at the Tyr^1–Gly^2 bond, which is responsible for 80% of the degradation pathway,[85,87] (ii) enkephalinase, cleaving the Gly^3-Phe^4 bond,[86] and (iii) dipeptidylaminopeptidase, cleaving the Gly^2–Gly^3 bond.[85] Accordingly, the development of inhibitors for these degrading enzymes is an important approach to the enhancement of analgesic activity by increasing the duration of the effect.

In the course of our study on the synthetic and medicinal chemistry of CF_3-containing amino acids, enzyme inhibitors and peptide hormones by exploring unique effects of the CF_3 group,[24,35,44,79] we designed and synthesized a series of novel enkephalin analogues bearing TFNV and TFNL. Then, their in vivo analgesic activity as well as in vitro receptor binding ability was examined.[88]

Synthesis of Novel Fluoro-enkephalin Analogues. A series of fluoro-enkephalin analogues was synthesized through solid-phase peptide synthesis by replacing either Gly^2 or Gly^3 by (*R*)-TFNV, (*S*)-TFNV, or (*R*)-TFNL, as shown in Scheme 10.[88] An analogue bearing (*N*-Me)Phe^4 in place of Phe^4 was also synthesized.

Scheme 10. Schematic Illustration of Modification Strategy of Methionine–Enkephalin with Trifluoronorvaline (TFNV) and Trifluoronorleucine (TFNL)

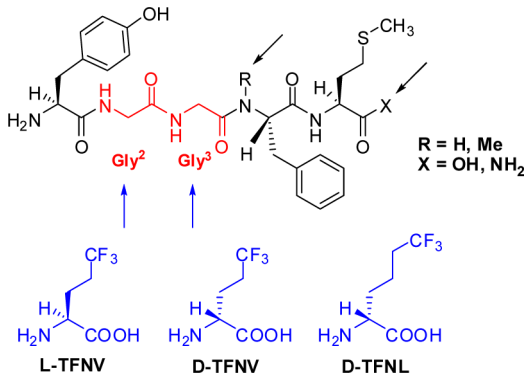

Analgesic Activity Assay in Vivo.[88] The in vivo analgesic activity of fluoro-enkephalin analogues was evaluated by the standard writhing test using ddY male mice via intracerebroventricular (i.c.v.) administration. As Table 2 shows, the substitution of Gly^2 by (*R*)-TFNV exhibited a remarkable increase in potency, i.e., 100000 times stronger than methionine–enkephalin, and even 1 order of magnitude stronger than morphine (entry 8). The absolute configuration of TFNV at this position is very important. Thus, [(*S*)-$TFNV^2$, Met^5-NH_2]enkephalin showed only ca. 30 times increase in potency (entry 7). The substitution of Gly^3 with TFNV improved potency by the factor of 30–60, in which the (*R*)-TFNV analogue was twice as effective as the (*S*)-TFNV analogue (entries 10, 11). The modification of carboxyl terminus to amide showed 5–6 times improvement in potency

dx.doi.org/10.1021/jo400301u | J. Org. Chem. 2013, 78, 6358–6383

Table 2. In Vivo Analgesic Activity of Fluoroenkephalin Analogs (i.c.v.)

entry	enkephalin	ED_{50} (10^{-9} mol/mouse)
1	methionine-enkephalin	700
2	morphine·HCl	0.07
3	Tyr-(*R*)-Ala-Gly-Phe-Met-NH_2	0.05
4	sedapain (morphine analogue)	0.05
5	Tyr-(*S*)-TFNV-Gly-Phe-Met	120
6	Tyr-Gly-(*S*)-TFNV-Phe-Met	140
7	Tyr-(*S*)-TFNV-Gly-Phe-Met-NH_2	25
8	Tyr-(*R*)-TFNV-Gly-Phe-Met-NH_2	0.007
9	Tyr-(*R*)-Nval-Gly-Phe-Met-NH_2	0.04
10	Tyr-Gly-(*S*)-TFNV-Phe-Met-NH_2	22
11	Tyr-Gly-(*R*)-TFNV-Phe-Met-NH_2	12
12	Tyr-(*R*)-TFNL-Gly-Phe-Met-NH_2	0.07
13	Tyr-(*R*)-TFNV-Gly-(N-Me)Phe-Met-NH_2	0.002

(entries 5, 6, 7, and 10). The substitution of Gly^2 with (*R*)-TFNL, a homologue of (*R*)-TFNV, exhibited 10000 times increase in potency, but it was 1 order of magnitude lower than the corresponding (*R*)-TFNV analogue (entry 12). The observed remarkable increase in potency for [(*R*)-$TFNV^2$, Met^5-NH_2]enkephalin was not entirely exceptional since a known analogue, [(*R*)-Ala^2, Met^5-NH_2]enkephalin, showed a 10000 fold increase in potency in the same in vivo assay (entry 3). In order to assess a "fluorine effect" on potency, (*R*)-norvaline ((*R*)-Nval) was synthesized and assayed. As entry 10 shows, this analogue exhibited almost equivalent potency to that of the (*R*)-Ala^2 analogue, which was 1 order of magnitude weaker than the (*R*)-TFNV analogue. Accordingly, it is clear that there was a "fluorine effect", which improved the potency by 1 order of magnitude even after a major enhancement factor, i.e., (*R*)-amino acid residue at Gly^2 position, was introduced. The most potent analogue in this series was [(*R*)-$TFNV^2$, (*N*-Me)Phe^4, Met^5-NH_2]enkephalin (entry 13), which was 3.5 times more potent than [(*R*)-$TFNV^2$, Met^5-NH_2]enkephalin.

Receptor Binding Assay in Vitro.[88] In order to investigate the origin of the remarkable enhancement in potency by the introduction of (*R*)-TFNV at the Gly^2 position, the in vitro receptor binding assays for [(*R*)-$TFNV^2$, Met^5-NH_2]enkephalin were carried out against μ, δ, and κ receptors using tritium-labeled standard ligands. As Table 2 shows, [(*R*)-$TFNV^2$, Met^5-NH_2]enkephalin exhibited a 10^{-10} M level IC_{50} against μ-receptor, but it was only a half order of magnitude enhancement in the binding ability compared with methionine-enkephalin. For δ-receptor, [(*R*)-$TFNV^2$, Met^5-NH_2]-enkephalin showed almost the same level binding ability as methionine−enkephalin. Interestingly, [(*R*)-$TFNV^2$, Met^5-NH_2]-enkephalin bound to the κ-receptor at the 10^{-7} M level IC_{50}, whereas methionine−enkephalin did not show any appreciable binding.

The results clearly indicate that the observed remarkable enhancement in the in vivo potency of [(*R*)-$TFNV^2$, Met^5-NH_2]enkephalin was not based on much stronger binding to receptor sites, but mainly due to the extremely efficient inhibition of degradation by aminopeptidase(s). Possible enhancement of the rates of absorption and transport, arising from the lipophilicity of CF_3 group should also be taken into account as the secondary effect. It is worth noting that [(*R*)-$TFNV^2$, Met^5-NH_2]enkephalin was found to cross the blood−brain barrier.

The studies described in this section clearly demonstrated the uniqueness and usefulness of fluoroamino acids as modifiers of peptides and enzyme inhibitors of medicinal interest. Thus, we envisioned that further research in this direction would explore newer and exciting aspects of organofluorine chemistry in medicinal chemistry and chemical biology.[89]

6. ENANTIOPURE FLUORINATED α-HYDROXY-β-AMINO ACIDS, THEIR DERIVATIVES, DIPEPTIDES, AND PEPTIDOMIMETICS

β-Amino acids have been attracting considerable interest because of their inherent biological activities and their useful characteristics as building blocks for potential therapeutic drugs and "β-peptides" with unique properties.[90,91] β-Amino acids are also useful for the studies of enzymatic reaction mechanisms.[90,91] Among various types of β-amino acids, α-hydroxy-β-amino acids (isoserines) are one of the most important members because many of them act as potent enzyme inhibitors and they also serve as crucial building blocks for the compounds of biological and medicinal importance.[91,92] For example, α-hydroxy-β-amino acid moieties are found in paclitaxel[93−95] (antitumor agent), bestatin[96,97] (inhibitor of aminopeptidases, immunological response modifier), amastatin[98] and phebestin[99] (aminopeptidase inhibitor), microginin[100] (ACE inhibitor, KNI inhibitor), and kinostatins (HIV-1 protease inhibitors)[101,102] (Figure 2).

In the last two decades, substantial research efforts have been made on the synthesis of fluorinated analogues of β-amino acids and investigation into their biological implications.[103−107] Because of the unique properties of fluorine as an element, the introduction of fluorine(s), CF_2H, or CF_3 group to biologically active molecules often critically improves their pharmacological properties.[19,103] Moreover, the sensitivity of ^{19}F NMR spec-

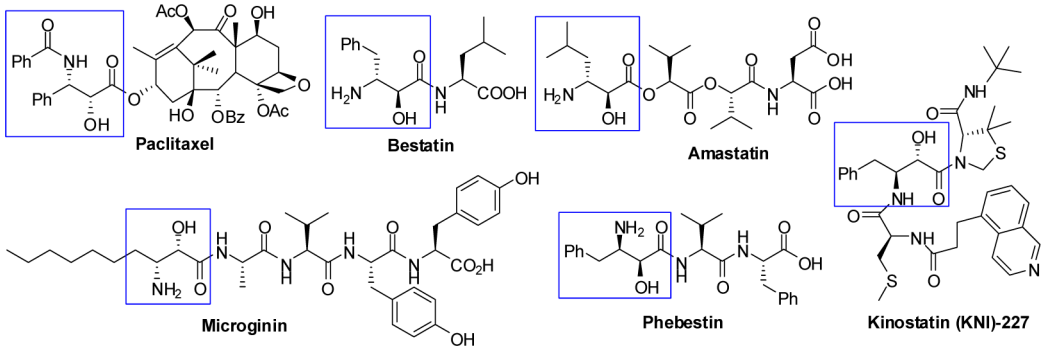

Figure 2. Representative biologically active compounds of medicinal interest bearing an α-hydroxy-β-amino acid residue.

dx.doi.org/10.1021/jo400301u | J. Org. Chem. 2013, 78, 6358−6383

troscopy along with large $^{19}F-^{1}H$ coupling constants and the virtual absence of ^{19}F in the living tissue render fluorine incorporation a particularly powerful tool for the investigation of biological processes.[8,108,109] Therefore, fluorine-containing α-hydroxy-β-amino acids are expected to serve as useful bioactive compounds with a wide range of potential applications in medicinal chemistry and chemical biology. However, only a few methods had been reported for the synthesis of fluorine-containing α-hydroxy-β-amino acids when we started our investigation in the mid-late 1990s.[19,110−114]

Accordingly, newer and efficient approaches to enantiopure fluorine-containing α-hydroxy-β-amino acids needed to be developed. To this end, the "β-lactam synthon method" invented in my laboratory and developed by us and others[115−120] offered an attractive protocol for the synthesis of enantiopure CF_2H- and CF_3-containing α-hydroxy-β-amino acids and their congeners.

6.1. Synthesis of Enantiopure 3-Hydroxy-4-CF_2H-β-lactams. Racemic *cis*-β-lactam (±)-**16** was prepared through [2 + 2] ketene−imine cycloaddition in good yield (Scheme 11).

Scheme 11. Preparation of Racemic 3-AcO-4-isobutenyl-β-lactam via Staundinger Ketene−Imine Cycloaddition and Its Subsequent Enzymatic Optical Resolution

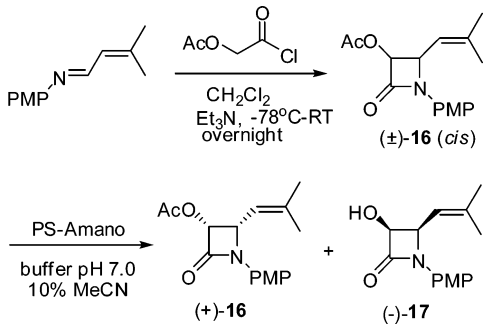

Then, the enzymatic optical resolution was carried out using the "PS-Amano" lipase.[121] This enzyme selectively hydrolyzes the acetate moiety of (−)-β-lactam (−)-**16** to afford kinetically resolved (3*R*,4*S*)-3-AcO-β-lactam (+)-**16** (>99% ee) and (3*S*,4*R*)-3-hydroxy-β-lactam (−)-**17** (96−99% ee) with extremely high enantiopurity in high recovery yields (Scheme 11).[122,123]

Since the acetyl group was not tolerated in the diethylaminosulfur trifluoride (DAST) reaction, the protecting group of the 3-hydroxyl moiety of β-lactam (+)-**16** was replaced with triisopropylsilyl (TIPS). The resulting 3-TIPSO-β-lactam (+)-**18** was subjected to ozonolysis to give 4-formyl-β-lactam (+)-**19**, which was immediately reacted with DAST to afford the corresponding 1-PMP-4-CF_2H-β-lactam (+)-**20** in high yield. Finally, the PMP group was removed using cerium ammonium nitrate (CAN) to give enantiopure (3*R*,4*R*)-3-TIPSO-4-CF_2H-β-lactam (+)-**21** (Scheme 12).[122,123] In a similar manner, (3*S*,4*S*)-3-hydroxy-β-lactam (−)-**17** was converted to enantiopure (3*S*,4*S*)-3-TIPSO-4-CF_2H-β-lactam (−)-**21**.

6.2. Synthesis of Enantiopure 3-Hydroxy-4-CF_3-β-lactams. A different strategy was employed for the synthesis of enantiopure 4-CF_3-β-lactams. Namely, the CF_3 moiety was introduced, from the very beginning, to the imine to be used for the [2 + 2] ketene−imine cycloaddition. *N*-PMP-trifluoroacetaldimine (**22**) was reacted with the ketene generated in situ

Scheme 12. Transformation of 3-AcO-4-isobutenyl-β-lactam to 3-TIPSO-4-CF_2H-β-lactam

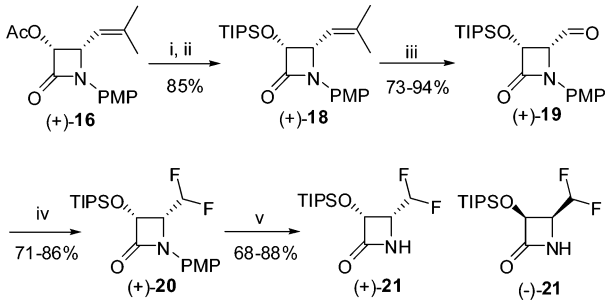

i) KOH, THF, 0 °C; ii) TIPSCl, Et_3N, DMAP; iii) O_3, $MeOH/CH_2Cl_2$, -78 °C; iv) DAST,CH_2Cl_2; v) CAN, H_2O/CH_3CN, -15 °C.

from benzyloxyacetyl chloride to afford racemic *cis*-3-BnO-4-CF_3-β-lactam (±)-**23** in moderate yield, as reported by us and others.[111,124] Hydrogenolysis of β-lactam (±)-**23**, followed by acetylation, gave the corresponding racemic *cis*-3-AcO-β-lactam (±)-**25** in good overall yield (Scheme 13).[122,123]

Scheme 13. Preparation of 4-AcO-4-CF_3-β-lactam via Staudinger Ketene−Imine Cycloaddition

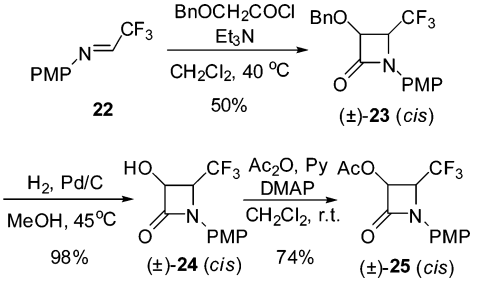

The enzymatic optical resolution of β-lactam (±)-**25** was performed using PS-Amano at 25 °C, pH 7 for 3 h (Scheme 14), which gave (3*R*,4*R*)-3-AcO-4-CF_3-β-lactam (+)-**25** with 99.9% ee as well as (3*S*,4*S*)-3-hydroxy-4-CF_3-β-lactam (-)-**26** with 97% ee in good to high yield.[122]

Scheme 14. Efficient Enzymatic Resolution of Racemic 3-AcO-F-CF_3-β-lactam

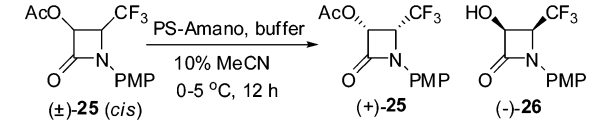

3-AcO-4-CF_3-β-lactam (+)-**25** and 3-hydroxy-4-CF_3-β-lactam (−)-**26**, thus obtained, were converted to the corresponding 3-TIPSO-4-CF_3-β-lactams, (+)-**28** and (−)-**28**, using the same protocol as that described for the preparation of (+)- and (−)-**21** (Scheme 15).[122,123]

6.3. Synthesis of Enantiopure 1-Acyl-3-hydroxy-4-R_f-β-lactams. The β-lactam synthon method has been developed by exploiting the unique nature of this strained four-membered skeleton for its facile ring-opening reactions with a variety of nucleophiles.[115,116] When the nitrogen of this strained cyclic amide is acylated (including carbalkoxy, carbamoyl, thiocarbamoyl, and sulfonyl groups besides the standard acyl groups), the resulting *N*-acyl-β-lactam becomes exceptionally reactive for

dx.doi.org/10.1021/jo400301u | J. Org. Chem. 2013, 78, 6358−6383

Scheme 15. Synthesis of (+)- and (−)-3-TIPS-4-CF_3-β-lactams

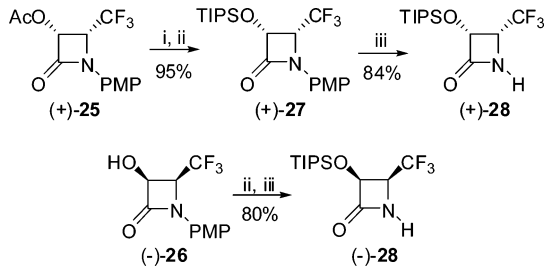

i) KOH, THF, -5 °C; ii) TIPSCl, Et_3N, CH_2Cl_2
iii) CAN, CH_3CN/H_2O, -10 °C.

nucleophilic attacks, leading to facile ring-opening coupling. This unique feature of *N*-acyl-β-lactams has been successfully utilized in organic synthesis and medicinal chemistry.[115,117−120]

We prepared a series of *N*-acyl-3-TIPSO-3-R_f-β-lactams **29** (R_f = CF_2H or CF_3), as examples, in good to high yield through acylation (including carbalkoxylation and sulfonylation) of 3-TIPSO-4-CF_2H-β-lactam **21** and 3-TIPSO-4-CF_3-β-lactam **28**, using $(Boc)_2O$, $ClCO_2Bn$, 4-F-C_6H_4COCl and *p*-$TolSO_2Cl$ in the presence of an appropriate base such as DMAP/Et_3N in CH_2Cl_2 (eq 17: only (3*R*,4*R*) series is shown for simplicity).[122,123]

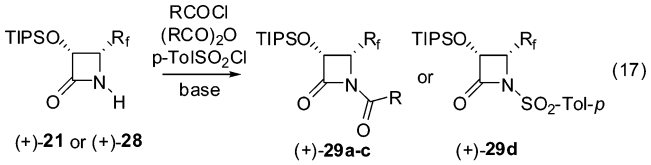

R_f = CF_2H or CF_3; R = t-BuO, BnO, 4-F-C_6H_4

6.4. Synthesis of Enantiopure β-CF_2H- and β-CF_3-α-hydroxy-β-amino Acids and Esters via Facile Hydrolysis/Alcoholysis of *N*-Acyl-β-lactams. Enantiopure β-R_f-α-hydroxy-β-amino acids (R_f = CF_2H or CF_3) were readily obtained through facile ring-opening hydrolysis of (+)- or (−)-**29**. For example, the reaction of 29 with KOH in aqueous THF at ambient temperature gave the corresponding *O*-protected amino acid **30**, in high yield (eq 18: only (2*S*,3*S*) series is shown for simplicity).[122,123] The *O*-TIPS protecting group could be easily removed by HF/pyridine as needed to give **31**.

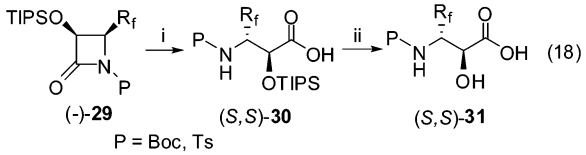

P = Boc, Ts
i) KOH, THF, H_2O, 25 °C, 12 h; ii) HF/pyr. 0 °C - r.t.

In a similar manner, enantiopure *O*-TIPS-β-R_f-α-hydroxy-β-amino acid methyl esters, (2*S*,3*S*)- or (2*R*,3*R*)-**32**, were obtained through a facile methanolysis of (+)- or (−)-**29** in the presence of Et_3N and a catalytic amount of DMAP at ambient temperature in good to quantitative yield (eq 19: only (2*R*,3*R*) series is shown for simplicity).[122,123] The *O*-TIPS protecting group could be easily removed by HF/pyridine as needed to give **33**.

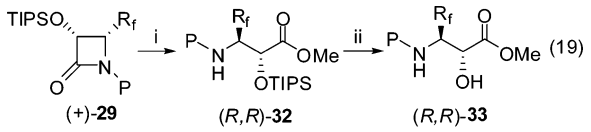

P = Boc, Cbz, Ts
i) MeOH, Et_3N, DMAP (cat.), 25 °C, 12 h; ii) HF/pyr. 0 °C - r.t.

6.5. Synthesis of R_f-Containing Isoserine Dipeptides through Efficient Ring-Opening Coupling of *N*-Acyl-β-lactams with α- and β-Amino Esters. The ring-opening coupling of *N*-acyl-β-lactam, (+)- or (−)-**36**, with various α- and β-amino acid esters provided a very easy access to a library of R_f-containing isoserine dipeptides. Since these coupling reactions do not need any peptide coupling reagents such as DCC, DIC and EDC, the "atom economy"[125] is extremely high. The coupling reactions gave the corresponding R_f-containing isoserine dipeptides, **34** and **35**, in good to quantitative yields (Scheme 16: Only (*S*,*S*,*S*) or (*S*,*S*) series is shown for simplicity).[122,123]

Scheme 16. Ring-Opening Coupling of 1-Acyl-4-R_f-β-lactams with α- and β-Amino Acid Esters

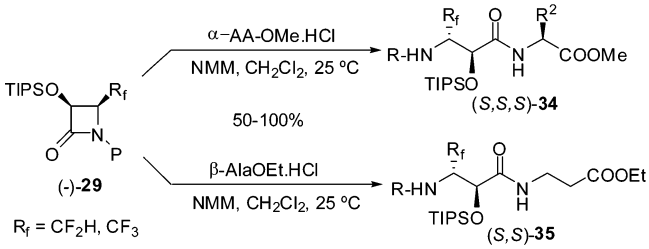

R_f = CF_2H, CF_3

P = Boc, Cbz, 4-F-Bz, Ts; R^2 = H, Me, $PhCH_2$, *i*-Pr, *i*-Bu, $MeS(CH_2)_2$

The results described above as well as our previous works[126−128] allow us to envision the versatile utility of the *N*-acyl-3-PO-4-R_f-lactams (P = hydroxyl protecting group) for the synthesis of R_f-containing isoserine dipeptides, depsipeptides, peptidomimetics, and key synthetic building blocks for R_f-containing hydroxyethylene, dihyroxylethylene, and hydroxyethylamine dipeptide isosteres. Possible transformations of *N*-carbalkoxy-3-PO-4-R_f-lactams are illustrated in Scheme 17.

Scheme 17. Feasible Transformations of 1-Carbalkoxy-4-R_f-β-lactams to Peptides and Peptidomimetics

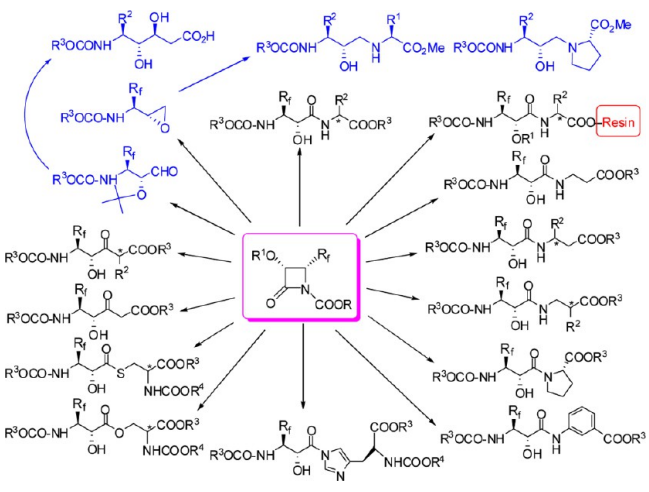

dx.doi.org/10.1021/jo400301u | J. Org. Chem. 2013, 78, 6358−6383

7. MEDICINAL CHEMISTRY AND CHEMICAL BIOLOGY OF FLUORINE-CONTAINING TAXOIDS

7.1. Paclitaxel and Taxoids. Paclitaxel (Taxol) and its semisynthetic analogue docetaxel (Figure 3) are two of the

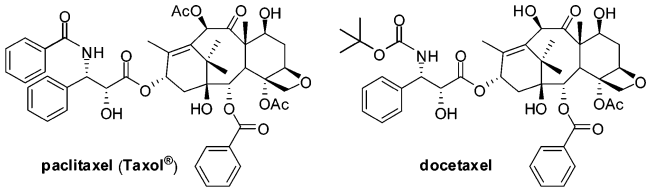

Figure 3. Chemical structures of paclitaxel and docetaxel.

most important chemotherapeutic drugs, currently used for the treatment of advanced ovarian cancer, metastatic breast cancer, melanoma, nonsmall cell lung cancer, and Kaposi's sarcoma.[129−131] More recently, these drugs have been used for the treatment of neck, prostate, and cervical cancers.[130,131] The mechanism of action of paclitaxel involves its binding to the β-subunit of α,β-tubulin dimer, accelerating the formation of microtubules. The resulting paclitaxel-bound microtubules are much more stable and less dynamic than the natural GTP-bound microtubules, with a growth rate higher than the disassembling rate. The unnatural growth and stabilization of microtubules causes the arrest of the cell division cycle mainly at the G2/M stage, activating a cell-signaling cascade that induces apoptosis.[132,133] Although paclitaxel and docetaxel possess potent antitumor activity, chemotherapy with these drugs encounters a number of undesirable side effects as well as drug resistance.[129−131] Therefore, it is important to develop new taxoid anticancer drugs as well as efficacious drug delivery systems with fewer side effects, superior pharmacological properties, and improved activity against various classes of tumors, especially against drug-resistant cancers.

7.2. The Fluorine Probe Approach: Solution-Phase Structure and Dynamics of Taxoids. The rational design of new generation taxoid anticancer agents would be greatly facilitated by the development of reasonable models for the biologically relevant conformations of paclitaxel. In this regard, we recognized that the design and synthesis of fluorine-containing taxoids would have a very useful offshoot of providing us with the capability of studying bioactive conformations of taxoids using a combination of $^{19}F/^{1}H$ NMR techniques and molecular modeling.[134]

The early conformational analysis of paclitaxel and docetaxel in solution largely identified two major conformations, with minor variations between studies.[135] Structure **I**, characterized by a gauche conformation with a H2′−C2′−C3′−H3′ dihedral angle of ca. 60°, was based on the X-ray crystal structure of docetaxel[136] and was believed to be commonly observed in aprotic solvents (Figure 4, I).[135] Structure **B**, characterized by the *anti* conformation with a H2′−C2′−C3′−H3′ dihedral angle of ca. 180°, was observed in theoretical conformational analysis[137,138] as well as 2D NMR analyses,[139] and found in the X-ray structure of the crystal obtained from a dioxane/H_2O/xylene solution (Figure 4, **II**).[140] Despite extensive structural studies, no systematic study on the dynamics of these two as well as other possible bioactive conformations of paclitaxel had been reported when we started our study on this problem. The relevance of the "fluorine probe" approach to study dynamic properties prompted us to conduct a detailed investigation into

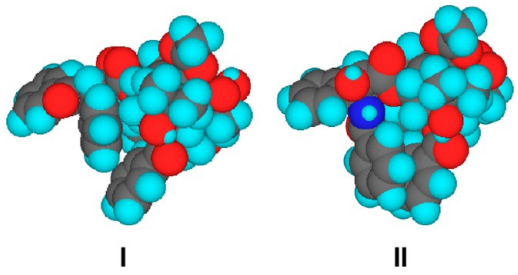

Figure 4. Paclitaxel conformations in aprotic solvent (**I**) and in aqueous solution (**II**).

the solution dynamics of fluorine-containing paclitaxel and docetaxel analogues.

The use of ^{19}F NMR for a variable temperature (VT) NMR study of fluorine-containing taxoids was obviously advantageous over the use of ^{1}H NMR because of the wide dispersion of the ^{19}F chemical shifts that allows fast dynamic processes to be frozen out. Accordingly, F_2-paclitaxel SB-T-31031 and F-docetaxel SB-T-3001 were selected as probes (Figure 5) for the study of the solution structures and dynamic behavior of paclitaxel and docetaxel, respectively, in protic and aprotic solvent systems.[134]

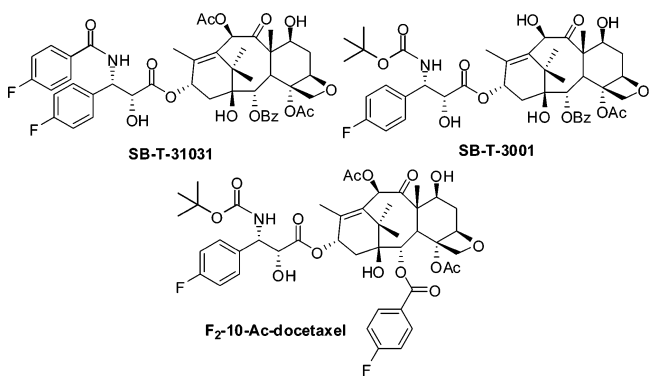

Figure 5. Paclitaxel and docetaxel fluorine probes for NMR analysis.

Analysis of the low temperature VT-NMR (^{19}F and ^{1}H) and $^{19}F-^{1}H$ heteronuclear NOE spectra of SB-T-31031 and SB-T-3001 in conjunction with molecular modeling revealed the presence of equilibrium between two conformers in protic solvent systems. Interpretation of the temperature dependence of the coupling constants between H2′ and H3′ for SB-T-31031 indicated that one of these conformers (conformer C, Figure 6 and Figure 7) possessed an unusual near-eclipsed arrangement around the H2′−C2′−C3′−H3′ dihedral angle ($J_{H2'-H3'}$ = 5.2 Hz, corresponding to the H2′−C2′−C3′−H3′ torsion angle of 124° based on the MM2 calculation) and was found to be more prevalent at ambient temperatures.[134] The other one corresponded to the *anti* conformer (conformer B, $J_{H2'-H3'}$ = 10.1 Hz, corresponding to the H2′−C2′−C3′−H3′ torsion angle of 178° based on the MM2 calculation) and was quite closely related to the structure **II** in Figure 4. These conformers were different from the one observed in aprotic solvents (conformer A, H2′−C2′−C3′−H3′ torsion angle of 54°) that was related to the X-ray crystal structure of docetaxel represented by the structure **I** in Figure 4.[136] Figure 6 shows the Newman projections for these three conformers and Figure 7 the structures of the conformers A, B, and C.[134]

dx.doi.org/10.1021/jo400301u | J. Org. Chem. 2013, 78, 6358−6383

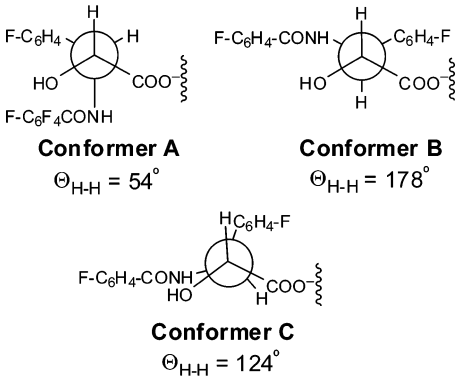

Figure 6. Newman projections of the isoserine moieties of the three conformers of F_2-paclitaxel identified.

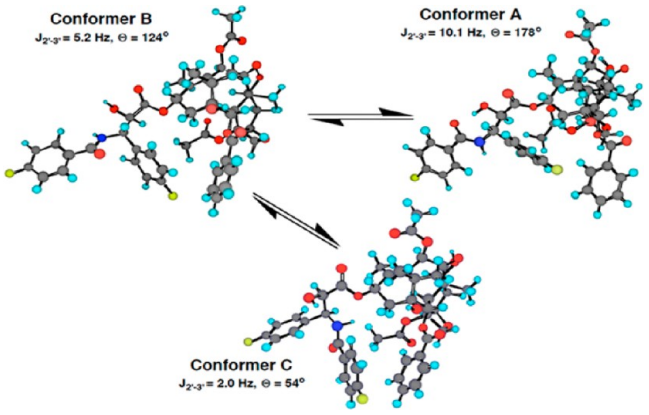

Figure 7. Three conformers of F2-paclitaxel identified.

Restrained molecular dynamics (RMD) studies presented evidence for the hydrophobic clustering of the 3′-phenyl and 2-benzoate (Ph moiety) for both conformers B and C. Although the conformer C possessed a rather unusual semieclipsed arrangement around the C2′−C3′ bond, the unfavorable interaction associated with such a conformation was apparently offset by significant solvation stabilization observed in the comparative RMD study in a simulated aqueous environment for the three conformers. The solvation stabilization term for the conformer C was estimated to be about 10 kcal/mol greater than those for the conformers A and B. Accordingly, the "fluorine probe" approach succeeded in finding a new conformer that had never been predicted by the previous NMR and molecular modeling studies.

Strong support for the conformer C was found in its close resemblance to a proposed solution structure of a water-soluble paclitaxel analog, paclitaxel-7-MPA (MPA = *N*-methylpyridinium acetate)[141] wherein the H2′−C2′−C3′−H3′ torsion angle of the *N*-phenylisoserine moiety is 127°, which is only a few degrees different from the value for the conformer C.

Thus, the "fluorine probe" approach has proved highly useful for the conformational analysis of paclitaxel and taxoids in connection with the determination of possible bioactive conformations. The previously unrecognized conformer C might be the molecular structure first recognized by the *β*-tubulin binding site on microtubules.

Determination of the Binding Conformation of Taxoids in Microtubules Using Fluorine Probes. The knowledge of the solution structures and dynamics of paclitaxel and its analogues is necessary for a good understanding of the recognition and binding processes between paclitaxel and its binding site on the microtubules. Such knowledge would also provide crucial information for the design of future generation anticancer agents. However, the elucidation of the microtubule-bound conformation of paclitaxel was critical for the rational design of efficient inhibitors of microtubule disassembly. The lack of information about the three-dimensional tubulin binding site by protein X-ray crystallography prompted us to apply our fluorine probe approach to the determination of the F−F distances in the microtubule-bound F_2-taxoids. The results of such a study should provide the relevant distance map for the identification of the bioactive (binding) conformation of paclitaxel.

We successfully applied the fluorine probe approach to the estimation of the F−F distance in the microtubule-bound F_2-10-Ac-docetaxel (Figure 5) using the solid-state magic angle spinning (SS MAS) ^{19}F NMR coupled with the radio frequency driven dipolar recoupling (RFDR) protocol in collaboration with L. Gilchrist, A. E. McDermott, K. Nakanishi (Columbia University), S. B. Horwitz, and M. Orr (A. Einstein College of Medicine).[107]

F_2-10-Ac-docetaxel was first studied in a polycrystalline form by the RFDR protocol. Based on the standard simulation curves derived from molecules with known F−F distances (distance markers), the F−F distance of two fluorine atoms in F_2-10-Ac-docetaxel was estimated to be 5.0 ± 0.5 Å (Figure 8). This

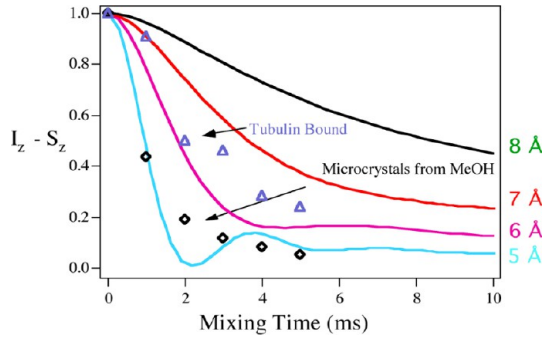

Figure 8. Determination of the F−F distance in F2-10-Ac-paclitaxel using the RFDR protocol by solid state MAS ^{19}F NMR spectroscopy.

value corresponded quite closely to the estimated F−F distances for the conformers B and C (F−F distance was ca. 4.5 Å for both conformers) based on our RMD studies for F_2-paclitaxel (SB-T-31031). This means that the microcrystalline structure of F_2-10-Ac-docetaxel was consistent with the hydrophobic clustering conformer B or C, but not with the conformer A in which the F−F distance was ca. 9.0 Å.

The microtubule-bound complex of F_2-10-Ac-docetaxel revealed the F−F distance to be 6.5 ± 0.5 Å (Figure 8), which was larger than that observed in the polycrystalline form by ca. 1 Å. It is very likely that the microtubule-bound conformation of F_2-10-Ac-docetaxel was achieved by a small distortion of the solution conformation, i.e., either conformer B or C.[107]

The above account demonstrated the power of the fluorine probe approach that is evident from its ability to supply extremely valuable and precise information about both bound and dynamic conformations of biologically active molecules. Such information is especially useful in the absence of knowledge about the three-dimensional crystal structure of their binding site. It is worthy of note that our preliminary study on the structure of the protein-bound fluorine-labeled

dx.doi.org/10.1021/jo400301u | J. Org. Chem. 2013, 78, 6358−6383

docetaxel, by means of the Solid State MAS ^{19}F NMR using the REDOR protocol, was the very first to tackle such an important and challenging problem in the structural and chemical biology of paclitaxel and tubulin/microtubules, which made a solid foundation for further investigations along this line (see section 7.6).

7.3. Second-Generation Taxoids. It has been shown that a primary mechanism of drug resistance is the overexpression of ABC transporters, e.g., P-glycoprotein, an integral membrane glycoprotein that acts as a drug-efflux pump to maintain the intracellular concentration of drugs below therapeutically active level.[142] In the course of our extensive studies on the design, synthesis and the structure−activity relationship (SAR) of taxoid anticancer agents, we discovered second-generation taxoids that possess 1 order of magnitude better activity against drug-sensitive cell lines and more than 2 orders of magnitude better activity against drug resistant cell lines.[143,144] Several examples are shown in Table 3 (see Figure 9 for structures). It

Table 3. In Vitro Cytotoxicity (IC_{50}, nM)[a] of Selected Second-Generation Taxoids

taxoid	MCF7[b]	NCI/ADR[c]	LCC6-WT[d]	LCC6-MDR[e]
paclitaxel	1.7	300	3.1	346
docetaxel	1.0	235	1.0	120
SB-T-1213	0.18	4.0		
SB-T-1103	0.35	5.1		
SB-T-121303	0.36	0.33	1.0	0.9
SB-T-121304	0.9	1.1	0.9	1.2
SB-T-11033	0.36	0.43	0.9	0.8

[a]The concentration of compound which inhibits 50% (IC_{50}, nM) of the growth of a human tumor cell line after 72 h drug exposure. [b]Human breast carcinoma. [c]Multidrug-resistant human ovarian cancer cell line. [d]Drug-resistance factor. [e]Multidrug-resistant human breast carcinoma.

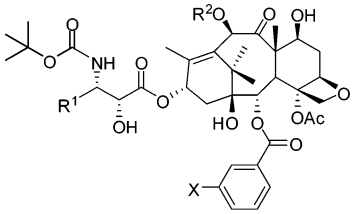

Figure 9. Selected second-generation taxoids.

was found that *meta*-substitution of the benzoyl group at the C2 position substantially increased the cytotoxicity of taxoids against drug-resistant cell lines.[144,145] This class of the second-generation taxoids is 3 orders of magnitude more potent than paclitaxel and docetaxel against drug-resistant cancer cell lines, expressing MDR phenotype (Table 3).[144,145]

Because of the aforementioned advantages of introducing fluorine into biologically active molecules, we synthesized fluorine-containing paclitaxel and docetaxel analogues to investigate the effects of fluorine−incorporation on the cytotoxicity and the blockage of known metabolic pathways.

7.4. 3′-Difluoromethyltaxoids and 3′-Trifluoromethyltaxoids. In the course of our extensive SAR studies of the taxoid anticancer agents, we have synthesized a good number of fluorotaxoids by means of the "*β*-lactam synthon method" to investigate the effects of fluorine on cytotoxicity and metabolic stability.[106,107,146] Along this line, second-generation fluorotaxoids possessing CF_2H and CF_3 groups at the 3′-position were synthesized and their biological activity evaluated.[122,147] The synthesis of these fluorotaxoids is shown in Scheme 18. The

Scheme 18. Synthesis of 3′-CF_2H- and 3′-CF_3-taxoids

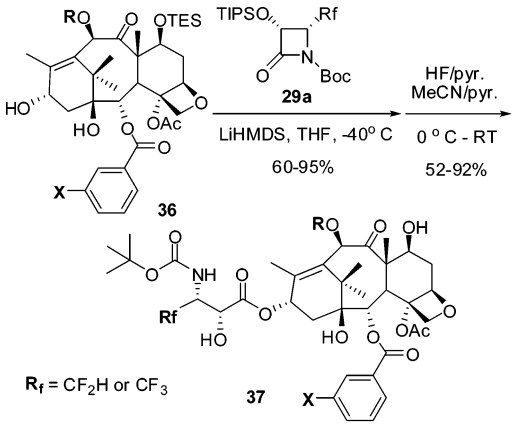

R = MeCO, EtCO, $N(Me)_2CO$, MeOCO,TES; **X** = MeO, F, Cl, N_3

Ojima−Holton coupling of (3*R*,4*R*)-1-Boc-4-CF_2H- and 1-Boc-4-CF_3-*β*-lactams **29a**, described above (see section 6.3), with 2,10-modified baccatins **36** was carried out at −40 °C in THF using LiHMDS as a base followed by removal of silicon protecting groups with HF/pyridine to give the corresponding second-generation 3′-CF_2H- and 3′-CF_3-taxoids **37** in moderate to high overall yields.

For the synthesis of CF_3-taxoids **38B** (R_f = CF_3), we also investigated a possible kinetic resolution of racemic *β*-lactam (±)-**29a-B** (R_f = CF_3) during the ring-opening coupling with enantiopure baccatin **36** under the standard conditions, except using 2.5 equivalents of racemic *β*-lactam.[148] As anticipated, we found a highly efficient kinetic resolution, affording CF_3-taxoids **37B** with diastereomer ratios of 9:1 to >30:1 (based on ^{19}F NMR analysis) in fairly good overall yields after deprotection. In three cases, only the single diastereomer of correct stereochemistry was obtained exclusively. The observed high level kinetic resolution of racemic 1-Boc-*β*-lactam (±)-**29a-B** by the lithium salt of the chiral secondary alcohol moiety at the 13-position of baccatin **37B** was nicely explained by the steric approach control using molecular modeling.

The cytotoxicity of selected fluorotaxoids against various cancer cell lines is shown in Table 4. These fluorotaxoids possess substantially higher potencies than those of paclitaxel and docetaxel against drug-sensitive cancer cell lines and their potency against multidrug-resistant cell lines is more impressive (2 orders of magnitude more potent than paclitaxel on average).[147]

7.5. 3′-Difluorovinyltaxoids. As described above, the introduction of isobutyl, isobutenyl, CF_2H, and CF_3 groups to the 3′-position of taxoids, replacing the phenyl group of paclitaxel and docetaxel, has led to the development of highly potent second-generation taxoids, especially against drug-resistant cancer cell lines, expressing MDR phenotype. Our

dx.doi.org/10.1021/jo400301u | J. Org. Chem. 2013, 78, 6358−6383

Table 4. In Vitro Cytotoxicity (IC_{50}, nM)[a] of Selected 3′-CF_2H- and 3′-CF_3-taxoids 37

taxoid	R_f	R	X	MCF7[b] (breast)	NCI/ADR[c] (ovarian)	R/S[d]	LCC6- WT[e] (breast)	H460[f] (lung)	HT-29[g] (colon)
paclitaxel				1.7	300	176	3.1	4.9	3.6
docetaxel				1.0	215	215			1.0
SB-T-12841-1	CF_2H	Ac	N_3	0.32	1.68	5.3	0.22	0.48	0.57
SB-T-12842-2	CF_2H	Et-CO	F	0.53	7.24	14	0.88	0.41	0.86
SB-T-12843-1	CF_2H	Me_2N-CO	MeO	0.45	4.51	10	0.69	0.40	0.43
SB-T-12844-3	CF_2H	MeO-CO	Cl	0.26	2.08	8.0	0.13	0.25	0.29
SB-T-12821-2	CF_3	Ac	F	0.45	5.58	13	0.38	0.49	1.11
SB-T-12822-4	CF_3	Et-CO	N_3	0.38	1.61	4.2	1.09	0.20	0.40
SB-T-12823-3	CF_3	Me_2NCO	Cl	0.12	1.02	8.5	0.27	0.42	0.45
SB-T-12824-1	CF_3	MeOCO	MeO	0.17	2.88	17	0.27	0.38	0.53

[a]Concentration of compound that inhibits 50% (IC_{50}, nM) of the growth of human tumor cell line after a 72 h drug exposure. [b]MCF7: human breast cancer cell line. [c]NCI/ADR: adriamycin-resistant human ovarian cancer cell line (Pgp+) (originally designated as "MCF7-R). [d]Resistance factor = (IC_{50} for drug resistant cell line, R)/(IC_{50} for drug-sensitive cell line, S). [e]LCC6-WT: human breast cancer cell line (Pgp-). [f]Human nonsmall cell lung cancer cell line. [g]Human colon cancer cell line.

metabolism studies on 3′-isobutyl- and 3′-isobutenyl-taxoids disclosed that the metabolism of second-generation taxoids (SB-T-1214 and SB-T-1103) was markedly different from that of docetaxel and paclitaxel.[149] These taxoids were metabolized (via hydroxylation) by CYP 3A4 of the cytochrome P450 family enzymes primarily at the two allylic methyl groups of the 3′-isobutenyl group and the methyne moiety of the 3′-isobutyl group (see Figure 10). This finding was in sharp contrast to the

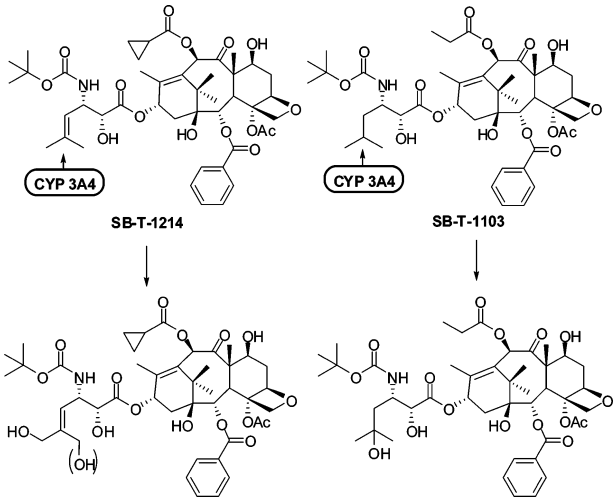

Figure 10. Primary sites of hydroxylation on the second-generation taxoids by cytochrome P450 family enzyme 3A4.

known result that the *tert*-butyl group of the C3′*N*-*t*-Boc moiety was the single predominant metabolic site for docetaxel.[150] These unique metabolic profiles prompted us to design and synthesize 3′-difluorovinyl-taxoids in order to block the allylic oxidation by CYP 3A4 mentioned above, which should enhance the metabolic stability and activity in vivo.

For the synthesis of a series of 3′-difluorovinyltaxoids **48**, novel (3*R*,4*S*)-1-*t*-Boc-3-TIPSO-4-difluorovinyl-*β*-lactam (+)-**47** was the key component for the coupling with baccatins **43** (Scheme 19).[151] We prepared *β*-lactam (+)-**47** in three steps from 4-formyl-*β*-lactam (+)-**26** (see Scheme 1) using the Wittig reaction of the formyl moiety with difluoromethylphosphorus ylide generated in situ from $(Me_2N)_3P/CF_2Br_2/Zn$ (Scheme 19).[151] The ring-opening coupling reaction of *β*-lactam (+)-**47** with baccatins **43** (X = H, MeO, N_3) and the subsequent removal of the silyl protecting groups gave the

Scheme 19. Synthesis of C3′-Difluorovinyltaxoids

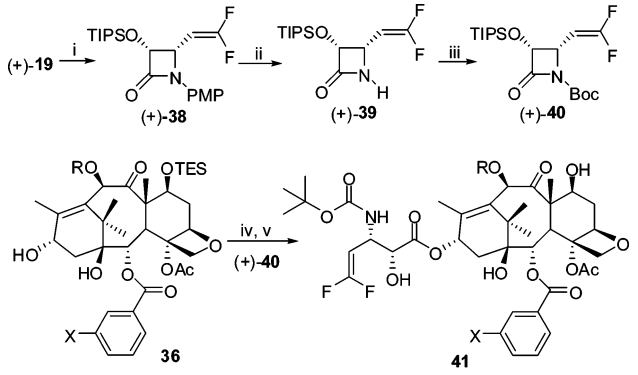

corresponding 3′-difluorovinyltaxoids **41** in good to excellent yields (Scheme 19).[151] Cytotoxicities of the 3′-difluorovinyltaxoids **41** were evaluated against 4 human cancer cell lines.[151,152] Results for selected taxoids are summarized in Table 5.

As Table 5 shows, all difluorovinyltaxoids **41** are exceedingly potent as compared to paclitaxel. A clear effect of C2-benzoate modification at the *meta* position (X = H vs X = MeO or N_3) was observed on the increase in potency against MCF7 (Pgp-) and NCI/ADR (Pgp+) cell lines (entries 2−5 vs entries 6−11). Difluorovinyltaxoids with 2,10-modifications (entries 6−11) exhibited impressive potency, exhibiting IC_{50} values in the <100 pM range (78−92 pM) except one case against MCF7 (entry 7) and in the subnanomolar range (0.34−0.57 nM) against NCI/ADR, which was 3 orders of magnitude more potent than paclitaxel. The resistance factor for these taxoids is 1.7−6.4, while that for paclitaxel is 250. Difluorovinyltaxoids with an unmodified C2-benzoate moiety (entries 2−5) also showed highly enhanced potency against MCF7 and NCI/ADR as compared to paclitaxel. These taxoids exhibited impressive potency against HT-29 (human colon) and PANC-1 (human pancreatic) cancer cell lines as well. SB-T-12853 appeared particularly promising against these gastrointestinal (GI) cancer cell lines.

7.6. Possible Bioactive Conformations of Fluorotaxoids. As described in section 7.2, we have successfully used fluorine-containing taxoids as probes for NMR analysis of the

dx.doi.org/10.1021/jo400301u | J. Org. Chem. 2013, 78, 6358−6383

Table 5. In Vitro Cytotoxicity (IC_{50}, nM)[a] of 3′-Difluorovinyltaxoids 41

entry	taxoid	R	X	MCF7[b] (breast)	NCI/ADR[c] (ovarian)	R/S	HT-29[d] (colon)	PANC-1[e] (pancreatic)
1	paclitaxel			1.2	300	250	3.6	25.7
2	SB-T-12851	Ac	H	0.099	0.95	9.6	0.41	1.19
3	SB-T-12852	c-Pr-CO	H	0.12	6.0	50	0.85	5.85
4	SB-T-12853	Et-CO	H	0.12	1.2	10	0.34	0.65
5	SB-T-12854	Me_2N-CO	H	0.13	4.3	33	0.46	1.58
6	SB-T-12852-1	c-Pr-CO	MeO	0.092	0.48	5.2		
7	SB-T-12853-1	Et-CO	MeO	0.34	0.57	1.7		
8	SB-T-12855-1	MeO-CO	MeO	0.078	0.50	6.4		
9	SB-T-12851-3	Ac	N_3	0.092	0.34	3.7		
10	SB-T-12852-3	c-Pr-CO	N_3	0.092	0.45	4.9		
11	SB-T-12855-3	MeO-CO	N_3	0.078	0.40	5.3		

[a−d]See footnotes of Table 3. [e]Human pancreatic carcinoma.

conformational dynamics of paclitaxel in conjunction with molecular modeling.[134] We have further applied the fluorine-probe protocol to the SS MAS ^{19}F NMR analysis with the RFDR method to measure the F−F distance in the microtubule-bound F_2-10-Ac-docetaxel.[107] Then, Schaefer and coworkers used the rotational echo double resonance (REDOR) to investigate the structure of the microtubule-bound paclitaxel by determining the $^{19}F-^{13}C$ distances of a fluorine-probe of paclitaxel (Figure 11).[153] These SS MAS ^{19}F NMR studies have provided critical information on the bioactive conformation of paclitaxel and docetaxel.

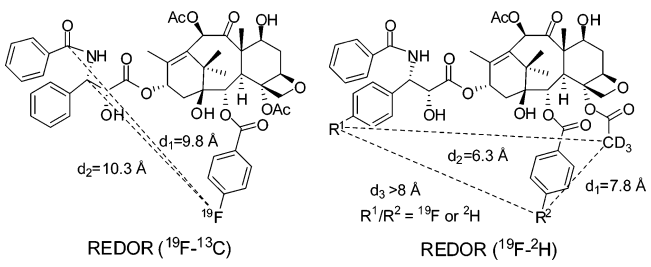

Figure 11. Solid-state NMR studies on microtubule-bound fluorotaxoid probes.

In 2005, we proposed a new bioactive conformation of paclitaxel, "REDOR-Taxol",[154] based on (i) the $^{19}F-^{13}C$ distances obtained by the REDOR experiment,[154] (ii) the photoaffinity labeling of microtubules,[155] (iii) the crystal structure (pdb code: 1TUB) of Zn^{2+}-stabilized α,β-tubulin dimer model determined by cryo-electron microscopy (cryo-EM),[156] and (iv) molecular modeling (Monte Carlo; Macromodel).[154] In this computational biology analysis, we docked a paclitaxel-photoaffinity label molecule to the position identified by our photoaffinity labeling study first and then optimized the position with a free paclitaxel molecule in the binding space using the REDOR distances as filters.[154]

In 2007, three additional intramolecular distances of the key atoms in the microtubule-bound $^{19}F/^{2}H$-labeled paclitaxel were determined by the REDOR method (Figure 11).[157] Also, it has been shown that the optimized cryo-EM crystal structure of tubulin-bound paclitaxel (pdb code: 1JFF)[158] serves better for the computational structure analysis. Accordingly, we have optimized our REDOR-Taxol structure, using the 1JFF coordinates as the starting point, by means of molecular dynamics simulations (Macromodel, MMFF94) and energy minimization (InsightII 2000, CVFF).[159]

We applied the same computational protocol to investigate the microtubule-bound structures of the 3′-CF_2H-, 3′-CF_3-, and 3′-CF_2C═CH-taxoids, using the updated REDOR-Taxol[159] as the starting structure. Three fluoro-taxoids, SB-T-1284, SB-T-1282, and SB-T-12853 (Figure 12), were docked into the

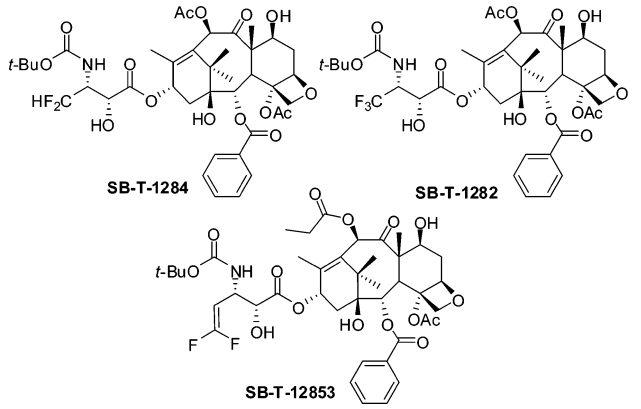

Figure 12. Three fluorotaxoids used for molecular modeling analysis.

binding pocket of paclitaxel in the β-tubulin subunit by superimposing the baccatin moiety with that of the REDOR-Taxol and their energies minimized (InsightII 2000, CVFF). The resulting computer-generated binding structures of three fluoro-taxoids are shown in Figure 13 (A, B, and C).[151]

As shown in Figure 13 (A, B, and C), the baccatin moiety occupies virtually the same space in all cases, as expected. Each fluorotaxoid fits comfortably in the binding pocket without any high-energy contacts with the protein. There is a very strong hydrogen bond between the C2′−OH of a fluorotaxoid and His^{229} of β-tubulin in all cases, which shares the same key feature with the REDOR-Taxol structure.[154] It should be noted that our preliminary study on the tubulin-bound structures of these three fluorotaxoids using the 1TUB coordinates led to different structures in which the C2′−OH had a hydrogen bonding to Arg^{359} of β-tubulin.[160] However, the use of the updated REDOR-Taxol structure based on the 1JFF coordinates unambiguously led to the fluoro-taxoids structures bearing a strong hydrogen bond between the C2′−OH and His^{229}.[151,152]

The CF_2H and CF_3 moieties fill essentially the same space, as anticipated. However, the CF_2C═CH moiety occupies more extended hydrophobic space than the CF_2H and CF_3 moieties. It is likely that this additional hydrophobic interaction is substantially contributing to the exceptional cytotoxicity of 3′-

dx.doi.org/10.1021/jo400301u | J. Org. Chem. 2013, 78, 6358−6383

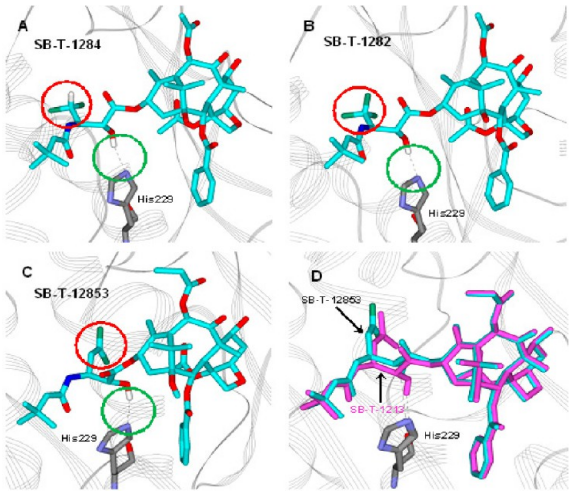

Figure 13. Computer-generated protein-bound structures of 3′-Rf-taxoids in β-tubulin 1JFF: (a) SB-T-1284 (3′-CF_2H); (b) SB-T-1282 (3′-CF_3); (c) SB-T-12853 (3′-CF_2═CH); (d) overlay of SB-T-12853 and SB-T-1213 (3′-isobutenyl).

difluorovinyltaxoids. The overlay of SB-T-12853 with a representative second-generation taxoid, SB-T-1213 shows very good fit, which may suggest that the difluorovinyl group mimics the isobutenyl group (Figure 13, D). However, the difluorovinyl group is in between the vinyl and isobutenyl groups in size, and two fluorine atoms may mimic two hydroxyl groups rather than two methyl groups electronically. Accordingly, the difluorovinyl group is a very unique structural component in medicinal chemistry and may serve as a versatile modifier of pharmacological properties in a manner similar to the trifluoromethyl group.

7.7. Use of Fluorine in Taxoid-Based Tumor-Targeting Anticancer Agents. Traditional chemotherapy depends on the premise that rapidly proliferating tumor cells are more likely to be destroyed by cytotoxic agents than normal cells. In reality, however, these cytotoxic agents have little or no specificity, which leads to systemic toxicity causing undesirable side effects. Accordingly, the development of tumor-specific drug delivery systems for anticancer agents, differentiating the normal tissues from cancer cells or tissues, is an urgent need to improve the efficacy of cancer chemotherapy. Various drug delivery systems have been studied over the past few decades to address this problem.[161] Rapidly growing cancer cells overexpress tumor-specific receptors to enhance the uptake of nutrients and vitamins. These receptors can be used as targets for cancer cell−specific delivery of cytotoxic agents through receptor-mediated endocytosis. Furthermore, the characteristic physiology of tumor and cancer cells can be exploited to selectively accumulate and release a cytotoxic agent inside these cells. Monoclonal antibodies, polyunsaturated fatty acids, folic acid, biotin, aptamers, transferrin, oligopeptides, and hyaluronic acid, for example, have been employed as tumor-specific "guiding modules" to construct tumor-targeting drug conjugates.[161−168]

As a general structure, tumor-targeted drug delivery systems consist of a tumor-targeting module (TTM) conjugated to a cytotoxic warhead directly or through a suitable "smart" linker (Figure 14). These drug conjugates should be stable in blood circulation to minimize systemic toxicity and should be effectively internalized inside the target tumor cells. Upon internalization, the drug conjugate should efficiently release the cytotoxic agent without loss of potency. Thus, the "smart" linkers should possess proper characteristics to provide suitable stability and reactivity.

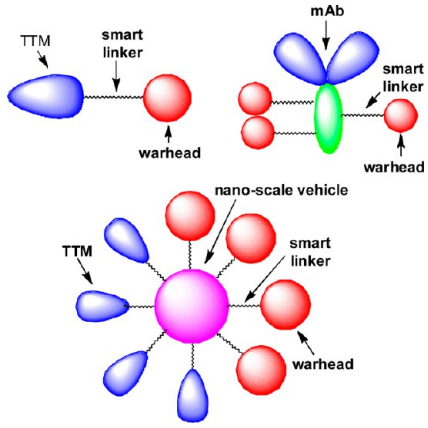

Figure 14. General structures of tumor-targeted drug delivery systems.

Fluorine-containing anticancer agents can certainly serve as potent "warheads" for the tumor-targeting drug conjugates.[104] In addition, fluorine can be strategically incorporated to create useful biochemical tools that facilitate the development of such tumor-targeting drug conjugates. For example, ^{19}F NMR can provide techniques to directly observe time-dependent processes in complex biological systems since the fluorine nucleus is virtually nonexistent in biological systems.[167] As ^{18}F is a common radioisotope used for positron emission tomography (PET) imaging, selective fluorination for biodistribution studies has found extensive use in diagnostic applications.[168−170]

This section concisely describes our recent approaches to the strategic incorporation of fluorine(s) into taxoid-based tumor-targeted drug delivery systems and ongoing investigations with future perspective.

7.7.1. Polyunsaturated Fatty Acid (PUFA)−Taxoid Conjugates. Omega-3 polyunsaturated fatty acids (PUFA), such as linolenic acid (LNA), eicosapentaenoic acid (EPA), and docosahexaenoic acid (DHA), are naturally occurring compounds found in vegetable oils, cold-water fish, and meat.[171] Perfusion studies have shown that some PUFAs are taken up more rapidly by tumor cells than normal cells.[172] It has also been shown that PUFAs are readily incorporated into cellular membranes, catabolized as an energy resource, and produce metabolites that act as signaling molecules, modulating various intracellular processes ranging from inflammatory response to cellular proliferation.[173] It has been shown that the conjugation of a drug to a PUFA greatly alters the pharmacokinetics (PK) profile of the parent compound, leading to tumor-selective accumulation of the drug conjugate.[174] Thus, a number of PUFA−drug conjugates are currently undergoing preclinical and clinical evaluations.[175] For example, DHA−paclitaxel (Taxoprexin), currently in phase III clinical trials, has exhibited better efficacy than paclitaxel in some studies[174,176] but does not show efficacy against multidrug-resistant (MDR) tumors that overexpress P-glycoprotein. As metioned above, second-generation taxoids and fluorotaxoids exhibited 2−3 orders of magnitude higher potency than paclitaxel against MDR cancer cell lines. Thus, PUFA conjugates, bearing a second-generation taxoid or fluorotaxoid should be more efficacious than DHA-paclitaxel against drug-resistant tumors.

Accordingly, novel DHA− and LNA−taxoid conjugates were synthesized and assayed in vivo for their efficacy against

dx.doi.org/10.1021/jo400301u | J. Org. Chem. 2013, 78, 6358−6383

different drug-resistant and drug-sensitive human tumor xenografts in severe combined immune deficiency (SCID) mice. Several of these conjugates led to a complete regression of the tumor in all surviving mice with minimal systemic toxicity. For example, DHA-SB-T-1214 led to a complete regression of the highly drug-resistant DLD-1 colon tumor xenograft in mice without appreciable systemic toxicity, wherein no recurrence of tumor growth was observed for more than 190 days after treatment.[177] DHA-SB-T-1214 is currently undergoing extensive late-stage preclinical evaluation, and an Investigational New Drug (IND) application will be filed to the US FDA in the near future. Since 3′-difluorovinyltaxoids exhibit equivalent or even higher potency than SB-T-1214 with excellent metabolic stability, DHA and LNA conjugates of SB-T-12854 (Figure 15) have been synthesized and their efficacy

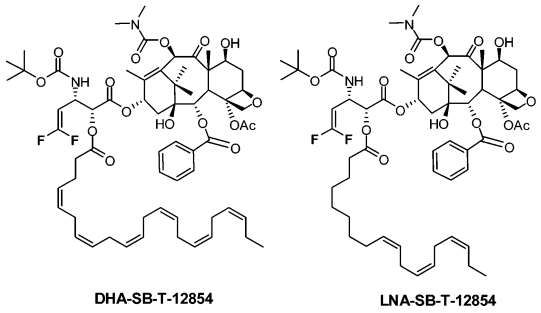

Figure 15. Omega-3 polyunsaturated fatty acid–fluorotaxoid conjugates.

in vivo is currently under active investigation. A preliminary in vivo efficacy study on LNA-SB-T-12854 against highly metastatic MX-1 human breast tumor xenograft in nude mice has shown promising results, wherein the complete eradication of tumor was achieved using weekly regimen for drug administration.

7.7.2. Self-Immolative Disulfide Linkers for Tumor-Targeted Drug Delivery. Monoclonal Antibody–Taxoid Conjugates with First-Generation Disulfide Linker. Cancer cells overexpress certain antigens on the cell surface and these tumor-specific antigens can be used as biomarkers to differentiate tumor tissues from normal tissues.[161,178,179] Certain monoclonal antibodies (mAb) have high binding specificity to tumor-specific antigens and can be used as drug delivery vehicles to carry a payload of cytotoxic agents specifically to the tumor site. The mAb–drug conjugate is internalized upon binding to the tumor antigen via receptor-mediated endocytosis (RME) and the payload is released inside the cancer cell. For example, brentuximab vedotin (Adcetris) is an mAb–drug conjugate targeting CD30 and recently approved by the FDA for the treatment of Hodgkin's lymphoma, and several other mAb–drug conjugates are currently in human clinical trials.[180,181]

The efficacy of mAb–drug immunoconjugates depends not only on the specificity of the mAb and the potency of the cytotoxic drug, but also on the linker which connects the mAb to the drug. We successfully conjugated a highly cytotoxic C-10 methyldisulfanylpropanoyl taxoid to immunoglobin G class mAbs, recognizing the epidermal growth factor receptor (EGFR), through a disulfide-containing linker (Figure 16).[182] These conjugates showed excellent selectivity in vitro and remarkable antitumor activity in vivo against A431 human squamous tumor xenografts in SCID mice, resulting in

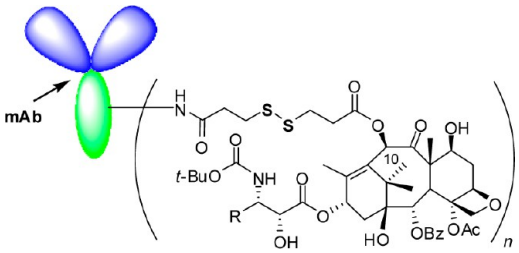

Figure 16. mAb–taxoid conjugate with first-generation disulfide linker.

eradication of the tumor without appreciable systemic toxicity.[182] However, the modification at the 10 position of the taxoid resulted in 8–10 times loss of potency relative to the parent taxoid.[182] Accordingly, the mechanism-based second-generation linker system was designed and developed to allow the release of the unmodified taxoid with uncompromised potency.

Second-Generation Self-Immolative Disulfide Linkers. Second-generation mechanism-based bifunctional disulfide linkers can be generally used to connect a warhead to one end and a tumor-targeting module (TTM) to the other end. This self-immolative disulfide linker module can release a taxoid warhead efficiently inside cancer cells by taking advantage of 1000 times higher concentration of glutathione in tumor as compared to that in blood plasma.[183] When the TTM navigates the drug-conjugate to the target receptors on the tumor surface, the whole conjugate is internalized via RME. Then, an intracellular thiol-triggered cascade drug-release takes place through thiolactonization (Figure 17) and the released potent

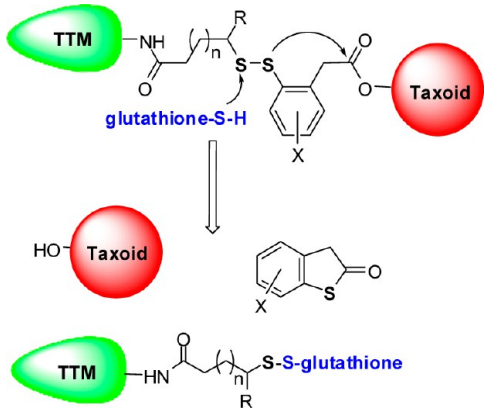

Figure 17. Second-generation self-immolative disulfide linker.

anticancer drug attacks its target protein, i.e., microtubules for taxoids. To promote the thiolactonization process, a phenyl moiety was strategically placed to direct the cleavage of the disulfide bond by intracellular thiol (e.g., glutathione), generating a thiophenolate or sulfhydrylphenyl species which attacks the ester linkage to the drug molecule (Figure 18).

The validity of this self-immolative drug-release mechanism has been proven in a model system using fluorine-labeling and monitoring by ^{19}F NMR spectroscopy (Figure 18)[104] as well as in a real system with cancer cells using fluorescence-labeling and confocal fluorescence microscopy (CFM).[184] These self-immolative disulfide linkers have been successfully incorporated into various tumor-targeting drug conjugates and their efficacy evaluated in cancer cells.[184−186]

dx.doi.org/10.1021/jo400301u | J. Org. Chem. 2013, 78, 6358−6383

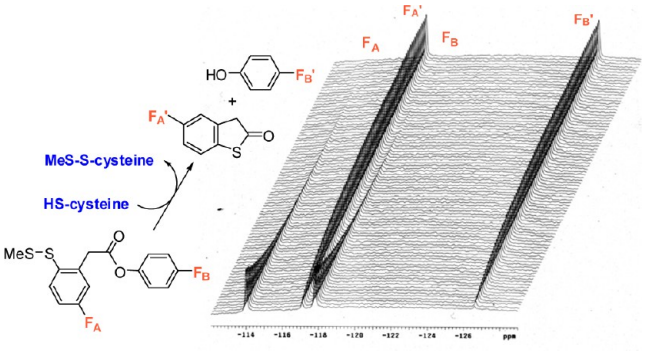

Figure 18. Time-dependent monitoring of disulfide cleavage and thiolactonization by ^{19}F NMR in a model system (adapted from ref 104. Copyright 2004 Wiley-VCH).

7.7.3. Vitamins as Tumor-Targeting Modules. Cancer cells critically require certain vitamins, such as those essential for cell division, to sustain their rapid growth although vitamins are essential for the growth and development of all living cells. Receptors for vitamins, including those for folic acid (vitamin M, vitamin B_9), biotin (vitamin H, vitamin B_7, coenzyme R), and vitamin B_{12}, are overexpressed on the cancer cell surface, providing useful targets for tumor-targeted drug delivery.[187] Among those vitamin receptors, folate receptors have been well-established and extensively studied as the target for drug delivery.[188] Biotin serves as a coenzyme for five biotin-dependent carboxylases and plays a significant role in epigenetic regulation, fatty acid synthesis, energy production and the metabolism of fats and amino acids.[189,190] Biotin receptors had not been studied until 2004 when vitamin receptor-targeted rhodamine polymers indicated that receptors for biotin were even more overexpressed on the surface of cancer cells than those for folic acid and vitamin B_{12}.[187] Thus, the biotin receptor has emerged as a novel target for tumor-targeted drug delivery in addition to the well-established folate receptors.

A general mechanism is illustrated in Figure 19 for the internalization of a tumor-targeting drug conjugate through receptor-mediated endocytosis (RME), drug release, and the binding of the released drug to the target protein (taxoid binds

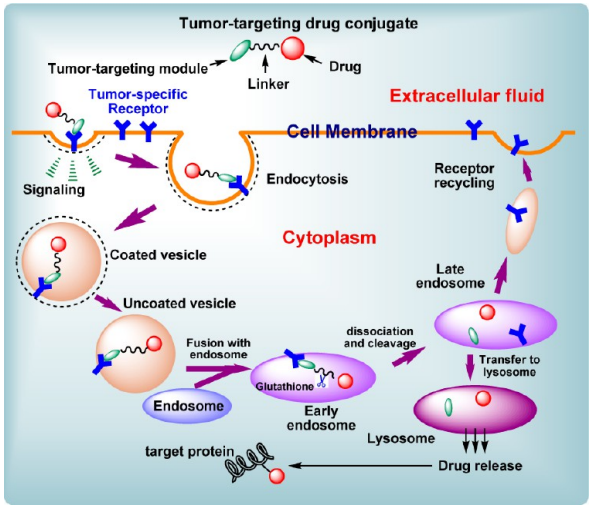

Figure 19. Schematic representation of the RME of a drug conjugate, drug release, and drug binding to the target protein (adapted from ref 186. Copyright 2010 American Chemical Society).

microtubules).[185] The internalization of the fluorescent probes via RME, drug release via disulfide bond cleavage and binding of the released taxoid "warhead" to microtubules were validated by CFM analysis of three fluorescent probes, i.e., (a) biotin–FITC conjugate, (b) biotin–linker–coumarin conjugate and (c) biotin–linker–taxoid(fluorescein).[166,184,186]

In addition, biotin–linker–taxoid conjugate was synthesized and assayed in vitro against L1210 (mouse lymphocytic leukemia), L1210FR (folate and biotin receptors overexpressed L1210 leukemia) and WI38 (normal human lung fibroblastoma) cells to examine the efficacy of the biomarker-specific targeting of the conjugate.[166,184,186] The IC_{50} values of the conjugate (taxoid = SB-T-1214) against L1210FR, L1210, and WI38 cell lines were 8.80 nM, 522 nM and 570 nM, respectively. The results clearly indicate the high target-specificity of the drug conjugate, which is consistent with the RME-based internalization and drug release observed by CFM and flow cytometry using fluorescent probes. Accordingly, this tumor-targeted drug delivery system bearing a vitamin as the tumor-targeting module is ready to utilize highly potent fluorotaxoids as "warheads".

Vitamin–linker–taxoid Conjugates Bearing an Imaging Arm for PET Analysis. As a part of our approach to developing taxoid-based novel "theranostics", i.e., combination of diagnostics and therapy, we designed vitamin–linker–taxoid conjugates bearing an imaging arm for PET analysis (Figure 20). In this novel drug conjugate, a vitamin TTM and taxoid

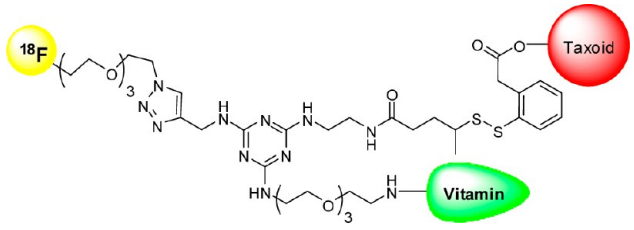

Figure 20. Vitamin–linker–taxoid conjugates bearing an imaging arm for PET analysis.

"warhead" are linked via a 1,3,5-triazine splitter with a water-solubilizing triethylene glycol (PEG_3) spacer and a self-immolative disulfide linker. The imaging arm is attached to the triazine splitter using click chemistry. The ^{18}F-(PEG_3)-moiety can be introduced either through the click reaction of ^{18}F-(PEG_3)-N_3 with the propargylaminotriazine conjugate or ^{18}F fluorination of the MsO-(PEG_3)-triazole linked to the triazine splitter in the drug conjugate, with Bu$N^{18}F$. For a feasibility study, we have successfully synthesized a prototype conjugate with a ^{19}F-(PEG_3)-arm, using biotin as TTM and SB-T-1214 as "warhead". The corresponding "hot" chemistry experiment will be performed in collaboration with the Fowler laboratory at the Brookhaven National Laboratory, shortly. Results of this radio-synthesis and biodistribution analysis of the tumor-targeting drug conjugate in real-time will be reported elsewhere in due course. Again, fluorotaxoids would serve as powerful "warheads" for these "theranostics" as well.

7.7.4. Nanoscale Vehicles for Tumor-Targeted Drug Delivery. Single-Walled Carbon Nanotubes as Vehicles for "Trojan Horse" Tumor-Targeted Drug Delivery. In the past decade, carbon nanotubes (CNTs) have emerged as a unique and efficient vehicle for transport and delivery of drugs.[191,192] Since functionalized carbon nanotubes (*f*-CNTs) were found

dx.doi.org/10.1021/jo400301u | J. Org. Chem. 2013, 78, 6358–6383

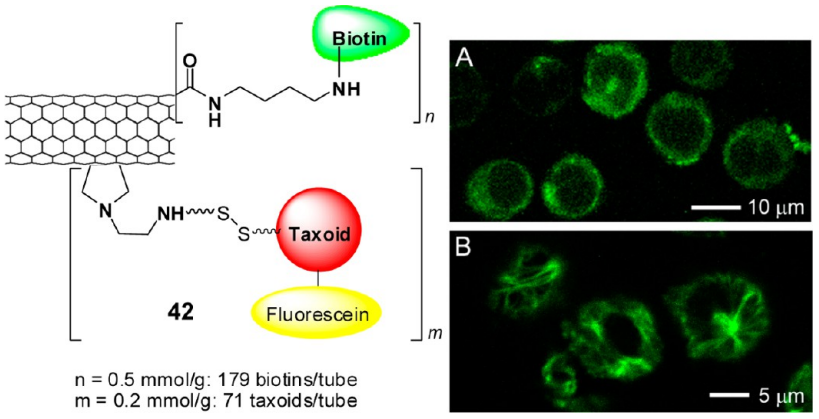

Figure 21. Novel SWNT-based tumor-targeting "Trojan Horse" drug conjugate **42** and the CFM images of L1210FR cells treated with **42** incubated (A) before and (B) after the addition of GSH-ethyl ester. Image B clearly highlights the presence of fluorescent microtubule networks in the living cells generated by the binding of taxoid–fluorescein upon cleavage of the disulfide bond in the linker by either GSH or GSH-ethyl ester. (CFM images adapted from ref 184. Copyright 2008 American Chemical Society).

to be nonimmunogenic and exhibit low toxicity, drug delivery systems using *f*-CNTs have been extensively studied.[191,192] We thought that single-walled carbon nanotubes (SWNTs) functionalized with vitamins as TTM would provide a nanoscale and biocompatible platform for tumor-targeted drug delivery. Thus, we designed and synthesized a novel biotin–SWNT–linker–taxoid(fluorescein) conjugate **42** (Figure 22) to investigate the mass-delivery of payloads to cancer cells, wherein the enhancement of internalization via RME was also expected through multivalent binding of TTM to the vitamin receptors.[184]

The internalization via RME, drug release and binding to the target protein (i.e., microtubules) of fluorescent SWNT–taxoid conjugate **42** were confirmed using CFM (Figure 21) and quantified by flow cytometry analysis using L1210FR cells.[184] The results were consistent with those for the biotin–linker–taxoid(fluorescein) conjugate mentioned above.

The cytotoxicity assay of the conjugate **42** against L1210FR, L1210 and WI38 cell lines (IC_{50} 0.36, >50, and >50 μg/mL, respectively) has revealed excellent target-specificity and substantially enhanced potency attributed to mass-delivery of the taxoid warheads inside the cancer cells. The results ensure the merit of the "Trojan Horse" strategy in tumor-targeting drug delivery.[184] This nanoscale drug delivery system is attractive for the tumor-specific delivery of highly potent fluorotaxoids. In addition to the use of a fluorotaxoid as "warhead", we plan to investigate possible monitoring of the drug release by ^{19}F NMR, using SWNT-taxoid conjugate **43** bearing a fluorine-containing self-immolative disulfide linker, wherein an unmodified "warhead" is used instead of fluorescein-tethered taxoid (Figure 22).

Asymmetric Bowtie Dendrimers As Vehicles for Tumor-Targeted Drug Delivery. Dendrimers are monodisperse, starburst polymers with a defined architecture originating from a central core. The high density of surface functional groups allows for polyvalent conjugation of TTMs, drugs, and tracers, which has made dendrimers highly versatile vehicles for tumor-targeted drug delivery, and extensive studies have been done.[193] Recently, an orthogonal diblock strategy for the generation of asymmetric bowtie dendrimers with a polyamido-(amine) (PAMAM) backbone and a cystamine core has been developed in our laboratory as well as by others.[194] First, two dendrimers are fully functionalized with TTMs, drugs or

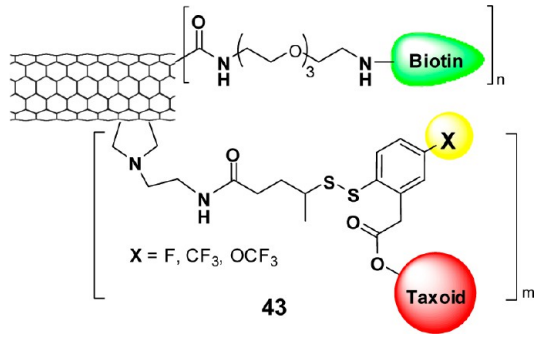

Figure 22. Novel SWNT-based tumor-targeting "Trojan Horse" drug conjugate **43** bearing a fluorine probe.

imaging agents. Second, each dendrimer is reductively cleaved to produce two half dendrons that can be asymmetrically joined *via* a bis-maleimido spacer. This synthetic approach offers unique advantages of selective modification and quantification of TTMs, drugs, and tracers on each half-dendron prior to coupling. Therefore, this strategy should produce tumor-targeting nanoscale drug conjugates with well-defined drug loading and enhanced tumor specificity.

We have designed a novel asymmetric bowtie dendrimer scaffold bearing a 1,3,5-triazine splitter in the bis-maleimide linker module to introduce an imaging module (Figure 23). We set out to construct a prototype dendrimer conjugate wherein the vitamin TTM is biotin, the "warhead" is fluorotaxoid SB-T-12854 or SB-T-1214, and the imaging module is fluorine (^{19}F for cold material and ^{18}F for PET). In this prototype, an asymmetric bow-tie dendrimer, consisting of the G3 and G1 PAMAM dendrons, is used. The G3 dendron allows the conjugation of 16 biotin molecules, while the G1 dendron holds 4 taxoids. We have successfully synthesized key components and the final assembly to the designed conjugate is in progress. Synthesis and biological evaluation of this dendrimer-based tumor-targeted drug delivery system will be reported in due course.

■ CONCLUDING REMARKS

This Perspective has covered the evolution of my research endeavor on fluorine chemistry not as a specialist in this field, but as an explorer of its interfaces with multidisciplinary fields

dx.doi.org/10.1021/jo400301u | J. Org. Chem. 2013, 78, 6358–6383

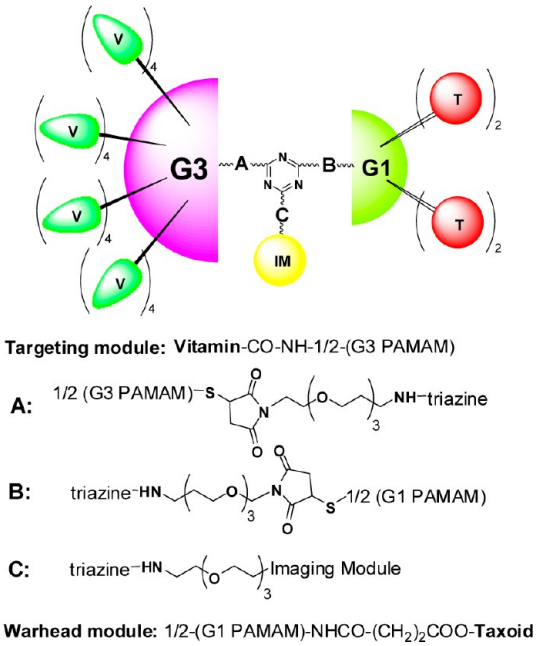

Figure 23. Tumor-targeted drug delivery system based on an asymmetric bowtie PAMAM dendrimer designed for the targeted delivery of second-generation taxoid/fluorotaxoid bearing an imaging arm.

in chemistry and biology. As mentioned, I was a synthetic chemist specializing in organometallic chemistry and homogeneous catalysis when I was brought into a very unique world of "fluorine chemistry" at the end of the 1970s. My laboratory started exploring the interface of fluorine chemistry and transition-metal catalysis, especially hydrocarbonylations and amidocarbonylation, which opened highly efficient synthetic routes to a variety of organofluorine compounds. Among them, CF_3-containing enantiopure amino acids were successfully applied to the enzyme inhibitor design, leading to the discovery of highly potent ACE inhibitor and enkephalin analogues. This line of research brought us into the field of medicinal chemistry. Also, trifluoromethacrylic acid was the key compound for the synthesis of trifluorothymine and this process was incorporated into the commercial process for the production of antiviral drug, trifluridine. We also introduced fluorine chemistry to the "β-lactam synthon method" and demonstrated the versatile and robust utility of fluorine-containing *N*-acyl-β-lactams as key intermediates to a library of fluorine-containing α-hydroxyl-β-amino acids and their peptides. Through expansion of this chemistry, we synthesized novel fluorine-containing taxoids and used them as excellent probes for the identification of bioactive conformations of paclitaxel and taxoids by means of ^{19}F NMR in solution and solid phase. We also designed and developed a series of fluorine-containing taxoids, which are highly potent in vitro and in vivo, especially against multidrug resistant tumors through strategic incorporation of fluorine for potency and metabolic stability. In the past decade, my laboratory has been developing new and efficacious tumor-targeted drug delivery systems for new generation cancer chemotherapy. These novel drug delivery systems consist of tumor-targeting modules, mechanism-based self-immolative disulfide linkers and warheads. Fluorotaxoids are obviously highly potent "warheads" for these tumor-targeting drug conjugates. In order to monitor the tumor-specific drug delivery, internalization, drug release, and drug binding to the target protein, we have been exploring the potential of the "fluorine probe" approach based on ^{19}F NMR as well as ^{18}F-tracer for PET analysis in addition to fluorescence-based probes. The use of multifunctionalized SWNTs as a drug delivery system bearing multiple-warheads and multiple-targeting modules has shown highly promising results on the benefit of mass-delivery ("Trojan Horse" strategy) of anticancer drug molecules to cancer cells with high specificity. We have also been constructing another nanosacle drug delivery system based on asymmetric bowtie PAMAM dendrimers, bearing an imaging module, including ^{18}F tracer for PET. Our future efforts will be concentrated on the design and synthesis of "tailor made nano-medicines" bearing imaging modules (for MRI, PET, fluorescence imaging and ^{19}F NMR), which would enable us to perform diagnostics and therapy in the real time.

Thus, my laboratory has been exploring the interfaces of fluorine chemistry and multidisciplinary field of research involving medicinal chemistry, chemical biology, cancer biology, and molecular imaging. When we explore new areas of research, naturally we enjoy and struggle with many "first" findings, successes, and problems. This is, to my opinion, the most exciting thing as a researcher.

AUTHOR INFORMATION

Corresponding Author

*E-mail: iwao.ojima@stonybrook.edu.

Notes

The authors declare no competing financial interest.

Biography

Iwao Ojima received his Ph.D. in organic chemistry from the University of Tokyo. He is currently a University Distinguished Professor and the Director of the Institute of Chemical Biology & Drug Discovery at Stony Brook University. His broad research program can be summarized as synthetic organic chemistry at the biomedical interface, including medicinal chemistry, organofluorine chemistry, and chemical biology.

ACKNOWLEDGMENTS

The author acknowledges numerous research grants from the National Institutes of Health (National Institute of General Medical Sciences and National Cancer Institute), National Science Foundation, and ACS Petroleum Research Fund, which have been supporting his research for the last three decades. Generous support from the New York State Science and Technology Foundation, Author C. Cope Fund, New York State Office of Science, Technology and Academic Research (NYSTAR), Rhone-Poulenc Rorer (now Sanofi), Indena SpA,

Mitsubishi Chemical Corp., Ajinomoto Co., Inc., Central Glass Co. Ltd., Japan Halon, Inc. (now Tohso F-Tech, Inc.), Tokyo Yuki Gosei Kogyo Co. Ltd., E. Merck, Darmstadt, and Fuji Chemical Ind. Co. Ltd. is acknowledged. The author also thanks his research group members at the Sagami Institute, who participated in the pioneering work on fluorine chemistry. He is grateful to all of his former and current graduate students, postdoctoral research associates, senior staff assistants, and staff of the Institute of Chemical Biology & Drug Discovery (ICB&DD), especially those who were engaged in the "fluorine chemistry" projects at Stony Brook, for their cooperation, support, and hard work, which made my endeavor fruitful. For the cover art, the author thanks Dr. Raphäel Geney for designing the background graphics, showing a tubulin-bound REDOR–Taxol molecule and a macrocyclic analogue, as well as Alexandra A. Athan for technical assistance to put together the images.

REFERENCES

(1) Begue, J.-P.; Bonnet-Delpon, D. *J. Fluorine Chem.* **2006**, *127*, 992.
(2) Isanbor, C.; O'Hagan, D. *J. Fluorine Chem.* **2006**, *127*, 303.
(3) Ojima, I. *Fluorine in Medicinal Chemistry and Chemical Biology*; Wiley-Blackwell: Chichester, 2009.
(4) Polina Cormier, E.; Das, M.; Ojima, I. In *Fluorine in Medicinal Chemistry and Chemical Biology*; Ojima, I., Ed.; Wiley-Blackwell: Chichester, 2009, p 525.
(5) *MedAdNews* **2007**, *13*, 200. See also: http://business.highbeam.com/437048/article-1G1-167388389/med-ad-news-200-bestselling-prescription-medicinescompanies.
(6) Müller, K.; Faeh, C.; Diederich, F. *Science* **2007**, *317*, 1881.
(7) O'Hagan, D.; Schaffrath, C.; Cobb, S. L.; Hamilton, J. T. G.; Murphy, C. D. *Nature* **2002**, *416*, 279.
(8) Martino, R.; Malet-Martino, M.; Gilard, V. *Curr. Drug Metab.* **2000**, *1*, 271.
(9) Wadhwani, P.; Strandberg, E. In *Fluorine in Medicinal Chemistry and Chemical Biology*; Ojima, I., Ed.; Wiley-Blackwell: Chichester, 2009, p 463.
(10) Kilbourn, M. R.; Shao, X. In *Fluorine in Medicinal Chemistry and Chemical Biology*; Ojima, I., Ed.; Wiley-Blackwell: Chichester, 2009, p 361.
(11) Uneyama, K. *Organofluorine Chemistry*; Blackwell: Oxford, 2006.
(12) Soloshonok, V. A. *Fluorine-Containing Synthons*; ACS Symposium Series 911; American Chemical Society: Washington, D.C., 2005.
(13) Soloshonok, V. A.; Mikami, K.; Yamazaki, T.; Welch, J. T.; Honek, J. F. *Current Fluoroorganic Chemistry: New Synthetic Directions, Technologies, Materials, and Biological Applications*; ACS Symposium Series 949; American Chemical Society: Washington, D.C., 2007; Vol. *949*.
(14) Kirsch, P. *Modern Fluoroorganic Chemistry: Synthesis, Reactivity, Applications*; Wiley–VCH: Stuttgart, 2004.
(15) Hiyama, T. *Organofluorine Compounds: Chemistry and Applications*; Springer–Verlag: Stuttgart, 2000.
(16) Soloshonok, V. A. *Enantiocontrolled Synthesis of Fluoroorganic Compounds: Stereochemical Challenges and Biomedicinal Targets*; Wiley: New York, 1999.
(17) Kitazume, T.; Yamazaki, T. *Experimental Methods in Organic Fluorine Chemistry*; Kodansha, Gordon and Breach Science Publisher: Tokyo, 1998.
(18) Hudlicky, M.; Pavlath, A. E. *Chemistry of Organic Fluorine Compounds II: A Critical Review*; American Chemical Society: Washington, D.C., 1995.
(19) Kukhar, V. P.; Soloshonok, V. A. *Fluorine-Containing Amino Acids: Synthesis and Properties*; Wiley: Chichester, 1994.
(20) Clark, L.; Gollan, R. *Science* **1966**, *152*, 1755.
(21) Ojima, I.; Tsai, C. Y.; Tzamarioudaki, M.; Bonafoux, D. In *Organic Reactions*; Overman, L. E., Ed.; Wiley: New York, 2000; Vol. *56*, p 1.
(22) Pino, P.; Piacenti, F.; Bianchi, M. In *Organic Syntheses via Metal Carbonyls*; Wender, I., Pino, P., Ed.; Wiley-Interscience: New York, 1977; Vol. *2*, p 43.
(23) Cornils, B. In *New Syntheses with Carbon Monoxide*; Falbe, J., Ed.; Springer-Verlag: Berlin, 1980; p 1.
(24) Ojima, I. *Chem. Rev.* **1988**, *88*, 1011.
(25) Filler, R. *Biochemistry Involving Carbon–Fluorine Bonds*; American Chemical Society: Washington, D.C., 1976.
(26) Filler, R. *CHEMTECH* **1973**, 752.
(27) Smith, F. A. *CHEMTECH* **1973**, 422.
(28) Filler, R., Kobayashi, Y. *Biomedical Aspects of Fluorine Chemistry*; Elsevier Biomedical: Amsterdam, 1982.
(29) Fuchikami, T.; Ojima, I. *J. Am. Chem. Soc.* **1982**, *104*, 3527.
(30) Ojima, I.; Kato, K.; Okabe, M.; Fuchikami, T. *J. Am. Chem. Soc.* **1987**, *109*, 7714.
(31) Ojima, I.; Fuchikami, T. U.S. Patent 4370504, 1983.
(32) Pino, P.; Piacenti, F.; Bianchi, M.; Lazzaroni, R. *Chim. Ind. (Milan)* **1968**, *50*, 106.
(33) Schwager, I.; Knifton, J. F. Ger. Offen. 2 322 751, 1973; *Chem. Abstr.* **1974**, *80*, 70327m.
(34) Booth, B. L.; Else, M. J.; Fields, R.; Haszeldine, R. N. *J. Organomet. Chem.* **1971**, *27*, 119.
(35) Ojima, I. *Actual. Chimique* **1987**, 171.
(36) Falbe, J. *New Syntheses with Carbon Monoxide*; Springer-Verlag: Berlin, 1980.
(37) Fuchikami, T.; Ohishi, K.; Ojima, I. *J. Org. Chem.* **1983**, *48*, 3803.
(38) Welch, J. T. *Tetrahedron* **1987**, *43*, 3123.
(39) Imperialli, B. In *Advances in Biotechnological Processes*; Mizrahi, A., Ed.; Alan R. Liss Inc.: New York, 1988; Vol. *10*, p 97.
(40) Imperialli, B.; Abeles, R. H. *Biochemistry* **1986**, *26*, 3760.
(41) Lamden, L.; Bartlett, P. A. *Biochem. Biophys. Res. Commun.* **1983**, *112*, 1085.
(42) Thaisrivongs, S.; Pals, D. T.; Kati, W. M.; Turner, S. R.; Thomasco, L. M.; Watt, M. *J. Med. Chem.* **1986**, *29*, 2080.
(43) Feuerstein, G.; Lozovsky, D.; Cohen, L. A.; Labroo, V. M.; Kirk, K.; Kopkin, I. J.; Faden, A. I. *Neuropeptides* **1984**, *4*, 303.
(44) Ojima, I.; Kato, K.; Nakahashi, K.; Fuchikami, T.; Fujita, M. *J. Org. Chem.* **1989**, *54*, 4511.
(45) Yamaguchi, S.; Mosher, H. S. *J. Org. Chem.* **1973**, *38*, 1870.
(46) Walborsky, H. M.; Baum, M.; Loncrini, D. F. *J. Am. Chem. Soc.* **1955**, *77*, 3637.
(47) Meng, H.; Clark, C. A.; Kumar, K. In *Fluorine in Medicinal Chemistry and Chemical Biology*; Ojima, I., Ed.; Wiley-Blackwell: Chichester, 2009; p 411.
(48) diPAMP = (1*R*,2*R*)-1,2-bis[(*o*-anisylphenyl)phosphino]ethane. See: Knowles, W. S.; Sabacky, M. J.; Vineyard, B. D.; Weinkauff, D. J. *J. Am. Chem. Soc.* **1976**, *97*, 2567.
(49) Fujita, M.; Ojima, I. *Tetrahedron Lett.* **1983**, *24*, 4573.
(50) Knorre, D. G.; Lavrik, O. I.; Petrova, T. D.; Savachenko, T. I.; Yakobson, G. G. *FEBS Lett.* **1971**, *12*, 204.
(51) Nevinsky, G. A.; Favorova, O. O.; Lavrik, O. I.; Petrova, T. D.; Kochkina, L. L.; Savachenko, T. I. *FEBS Lett.* **1974**, *43*, 135.
(52) Pless, S. A.; Galpin, J. D.; Niciforovic, A. P.; Ahern, C. A. *Nature Chem. Biol.* **2011**, *7*, 617.
(53) Budisa, N. *Engineering the Genetic Code*; Wiley-VCH: Weinheim, 2006.
(54) Henne, A. L.; Naer, M. J. *J. Am. Chem. Soc.* **1951**, *73*, 1042.
(55) Fuchikami, T.; Yamanouchi, A.; Ojima, I. *Synthesis* **1984**, 766.
(56) Ito, H.; Miller, D. C.; Willson, C. G. *Macromolecules* **1982**, *15*, 915.
(57) Koishi, T.; Tanaka, I.; Yasumura, T.; Ojima, I.; Fuchikami, T. Jpn. Patent 1676867, 1992.
(58) Ojima, I.; Fuchikami, T. Jpn. Patent 1418495, 1988.
(59) Ojima, I.; Fuchikami, T. Jpn. Patent 1640707, 1992.

(60) Ito, H.; Truong, H. D.; Okazaki, M.; Miller, D. C.; Fender, N.; Brock, P. J.; Wallraff, G. M.; Larson, C. E.; Allen, R. D. *J. Photopolym. Sci. Technol.* **2002**, *15*, 591.
(61) Shirai, M.; Takashiba, S.; Tsunooka, M. *J. Photopolym. Sci. Technol.* **2003**, *16*, 545.
(62) Cracowski, J.-M.; Montembault, V.; Hardy, I.; Bosc, D.; Améduri, B.; Fontaine, L. *J. Polym. Sci. A - Polym. Chem.* **2008**, *46*, 4383.
(63) Ojima, I.; Nakahashi, K. *Japan Kokai Tokkyo Koho* **1990**, *Hei 4*, 49298.
(64) Ojima, I.; Nakahashi, K. U.S. Patent 5276137, 1994.
(65) Schoenberg, A.; Heck, R. F. *J. Org. Chem.* **1974**, *39*, 3327.
(66) Fuchikami, T.; Ojima, I. *Tetrahedron Lett.* **1982**, *23*, 4099.
(67) Heidelberger, C.; Barsons, D. G.; Remy, D. C. *J. Am. Chem. Soc.* **1962**, *84*, 3597.
(68) Ojima, I.; Fuchikami, T. Jpn. Patent 1634611, 1992.
(69) O'Brien, W.; Taylor, J. *Invest. Ophthalmol. Vis. Sci.* **1991**, *32*, 2455.
(70) Ojima, I.; Okabe, M.; Kato, K.; Kwon, H. B.; Horvlth, I. T. *J. Am. Chem. Soc.* **1988**, *210*, 150.
(71) Horváth, I. T.; Bor, G.; Garland, M.; Pino, P. *Organometallics* **1986**, *5*, 1441.
(72) Bor, G. *Pure Appl. Chem.* **1986**, *58*, 543.
(73) Spindler, F.; Bor, G.; Dietler, U.; Pino, P. *J. Organomet. Chem.* **1981**, *213*, 303.
(74) Cushman, D. W.; Cheung, H. S.; Sabo, E. F.; Ondetti, M. A. *Biochemistry* **1977**, *16*, 5484.
(75) Ondetti, M. A.; Rubin, B.; Cushman, D. W. *Science* **1977**, *196*, 441.
(76) Patchett, A. A.; Harris, E.; Tristram, E. W.; Wyvratt, M. J.; Taub, D.; Peterson, E. R.; Ikeler, T. J.; ten Broeke, J.; Payne, L. G.; Ondeyka, D. L.; Thorsett, E. D.; Greenlee, W. J.; Lohr, N. S.; Hoffsommer, R. D.; Joshua, H.; Ruyle, W. V.; Rothrack, J. W.; Aster, S. D.; Maycock, A. L.; Robinson, F. M.; Hirschmann, R.; Sweet, C. S.; Ulm, E. H.; Gross, D. M.; Vassil, T. C.; Stone, C. A. *Nature* **1980**, *288*, 280.
(77) Filler, R. *J. Fluorine Chem.* **1986**, *33*, 361.
(78) Ojima, I.; Jameison, F. A.; Peté, B.; Radunz, H.; Schittenhelm, C.; Lindner, H. J.; Smith, A. *Drug Design Discov.* **1994**, *11*, 91.
(79) Ojima, I.; Jameison, F. A. *Bioorg. Med. Chem. Lett.* **1991**, *1*, 581.
(80) Holmquist, B.; Bunning, P.; Riordan, J. F. *Anal. Biochem.* **1979**, *95*, 540.
(81) Smith, A. E.; Lindner, H. J. *J. Computer-Aided Mol. Design* **1991**, *5*, 235.
(82) Hansen, P. E.; Morgan, B. A. In *The Peptides – Analysis, Synthesis, Biology; Vol 6. Opioid Peptides: Biology, Chemistry, and Genetics*; Undenfriend, S., Meienhofer, J., Eds.; Academic Press: Waltham, 1984; p 269.
(83) Paterson, S. J.; Robson, L. E.; Kosterlitz, H. W. In *The Peptides – Analysis, Synthesis, Biology; Vol 6. Opioid Peptides: Biology, Chemistry, and Genetics*; Undenfriend, S., Meienhofer, J., Eds.; Academic Press: Waltham, 1984; p 147.
(84) Watanabe, J.; Tokuyama, S.; Takahashi, M.; Kaneto, H.; Maeda, M.; Kawasaki, K.; Taguchi, T.; Kobayashi, Y.; Yamamoto, Y.; Shimokawa, K. *J. Pharmacobio-Dyn.* **1991**, *14*, 101.
(85) Thorsett, E. D.; Wyvratt, M. J. In *Neuropeptides and Their Peptidases*; Turner, A. J., Ed.; Ellis Horwood-VCH: Chichester, 1987; p 229.
(86) Turner, A. J. In *Neuropeptides and Their Peptidases*; Turner, A. J., Ed.; Ellis Horwood-VCH: Chichester, 1987; p 183.
(87) McKelvy, J. F. *Annu. Rev. Neurosci.* **1986**, *9*, 415.
(88) Ojima, I.; Jameison, F. A.; Conway, J. D.; Nakahashi, K.; Hagiwara, M.; Miyamae, T.; Radunz, H. E. *Bioorg. Med. Chem. Lett.* **1992**, *2*, 219.
(89) Ojima, I. In *Organofluorine Compounds in Medicinal Chemistry and Biomedical Applications*; Filler, R., Kobayashi, Y., Yagupolskii, L. M., Eds.; Elsevier: Amsterdam, 1993, p 241.
(90) Juaristi, E. *Enantioselective Synthesis of β-Amino Acids*: Wiley-VCH: New York, 1997.
(91) Cole, D. C. *Tetrahedron* **1994**, *50*, 9517.
(92) Ojima, I.; Delaloge, F. In *Peptidomimetics Protocols*; Kamierski, W., Ed.; Humana Press: New York, 1998, p 137.
(93) Kingston, D. G. I. *Chem. Commun.* **2001**, *10*, 867.
(94) Ojima, I.; Lin, S.; Wang, T. *Curr. Med. Chem.* **1999**, *6*, 927.
(95) Georg, G. I.; Chen, T. T.; Ojima, I.; Vyas, D. *Taxane Anticancer Agents: Basic Science and Current Status*; American Chemical Society: Washington D.C., 1995; Vol. *583*.
(96) Umezawa, H.; Aoyagi, T.; Suda, H.; Hamada, M.; Takeuchi, T. *J. Antibiot.* **1976**, *29*, 97.
(97) Pearson, W. H. H. *J. Org. Chem.* **1989**, *54*, 4235.
(98) Roers, R.; Verdine, G. L. *Tetrahedron Lett.* **2001**, *42*, 3563.
(99) Nagai, M.; Kojima, F.; Naganawa, H.; Hamada, M.; Aoyagi, T.; Takeuchi, T. *J. Antibiot.* **1997**, *50*, 82.
(100) Okino, T.; Matsuda, H.; Murakami, M.; Yamaguchi, K. *Tetrahedron Lett.* **1993**, *34*, 501.
(101) Mimoto, T.; Hattori, N.; Takaku, H.; Kisanuki, S.; Fukazawa, T.; Terashima, K.; Kato, R.; Nojima, S.; Misawa, S.; Ueno, T.; Imai, J.; Enomoto, H.; Tanaka, S.; Sakikawa, H.; Shintani, M.; Hayashi, H.; Kiso, Y. *Chem. Pharm. Bull.* **2000**, *48*, 1310.
(102) Kiso, Y.; Matsumoto, S.; Mimoto, H.; Kato, T.; Nojima, R.; Takaku, S.; Fukazawa, H.; Kimura, T.; Akaji, T. *Arch. Pharm.* **1998**, 87.
(103) Ojima, I.; McCarthy, J. M.; Welch, J. T. *Biomedical Frontiers of Fluorine Chemistry, ACS Symp. Series 639*; American Chemical Society: Washington, D.C., 1996.
(104) Ojima, I. *ChemBioChem* **2004**, *5*, 628.
(105) Hook, D. F.; Gessier, F.; Noti, C.; Kast, P.; Seebach, D. *ChemBioChem* **2004**, *5*, 691.
(106) Ojima, I.; Inoue, T.; Chakravarty, S. *J. Fluorine Chem.* **1999**, *97*, 3.
(107) Ojima, I.; Inoue, T.; Slater, J. C.; Lin, S.; Kuduk, S. C.; Chakravarty, S.; Walsh, J. J.; Gilchrist, L.; McDermott, A. E.; Cresteil, T.; Monsarrat, B.; Pera, P.; Bernacki, R. J. In *Asymmetric Fluoroorganic Chemistry: Synthesis, Application, and Future Directions*; ACS Symposium Series 746; Ramachandran, P. V., Ed.; American Chemical Society: Washington, D.C., 1999, p 158.
(108) O'Hagan, D.; Schaffrath, C.; Cobb, S. L.; Hamilton, J. T. G.; Cormac, D.; Murphy, C. D. *Nature* **2002**, *416*, 279.
(109) Gerhard, U.; Thomas, S.; Mortishire-Smith, R. *J. Pharm. Biol. Anal.* **2003**, *32*, 531.
(110) Kaneko, S.; Yamazaki, T.; Kitazume, T. *J. Org. Chem.* **1993**, *58*, 2302.
(111) Abouabdellah, A.; Begue, J. P.; Bonnet-Delpon, D.; Nga, T. T. T. *J. Org. Chem.* **1997**, *62*, 8826.
(112) Uneyama, K.; Hao, J.; Amii, H. *Tetrahedron Lett.* **1998**, *39*, 4079.
(113) Soloshonok, V. A.; Soloshonok, I. V.; Kukhar, V. P.; Svedas, V. K. *J. Org. Chem.* **1998**, *63*, 1878.
(114) Fustero, S.; Pina, B.; Salavert, E.; Navarro, A.; Ramírez de Arellano, M. C.; Simón Fuentes, A. *J. Org. Chem.* **2002**, *67*, 4667.
(115) Ojima, I. *Acc. Chem. Res.* **1995**, *28*, 383.
(116) Ojima, I.; Delaloge, F. *Chem. Soc. Rev.* **1997**, *26*, 377.
(117) Deshmukh, A. R.; Bhawal, B. M.; Krishnaswamy, D.; Govande, V. V.; Shinkre, B. A.; Jayanthi, A. *Curr. Med. Chem.* **2004**, *11*, 1889.
(118) Alcaide, B.; Almendros, P. *Curr. Med. Chem.* **2004**, *11*, 1921.
(119) Palomo, C.; Aizpurua, J. M.; Ganboa, I.; Oiardide, M. *Curr. Med. Chem.* **2004**, *11*, 1837.
(120) Kamath, A.; Ojima, I. *Tetrahedron* **2012**, *68*, 10640.
(121) Brieva, R.; Crich, J. Z.; Sih, C. J. *J. Org. Chem.* **1993**, *58*, 1068.
(122) Kuznetsova, L.; Ungureanu, I. M.; Pepe, A.; Zanardi, I.; Wu, X.; Ojima, I. *J. Fluorine Chem.* **2004**, *125*, 487.
(123) Ojima, I.; Kuznetsova, L.; Ungureanu, I. M.; Pepe, A.; Zanardi, I.; Chen, J. In *Fluorine-Containing Synthons*; ACS Symposium Series 911; Soloshonok, V. A., Ed.; American Chemical Society/Oxford University Press: Washington, D.C., 2005, p 544.
(124) Ojima, I.; Slater, J. C.; Pera, P.; Veith, J. M.; Abouabdellah, A.; Begue, J.-P.; Bernacki, R. J. *Bioorg. Med. Chem. Lett.* **1997**, *7*, 133.
(125) Trost, B. M. *Acc. Chem. Res.* **2002**, *35*, 695.
(126) Ojima, I.; Sun, C. M.; Park, Y. H. *J. Org. Chem.* **1994**, *59*, 1249.

(127) Ojima, I.; Wang, T.; Delaloge, F. *Tetrahedron Lett.* **1998**, *39*, 3663.
(128) Ojima, I.; Wang, T.; Ng, E. W. *Tetrahedron Lett.* **1998**, *39*, 923.
(129) Rowinsky, E. K. *Annu. Rev. Med.* **1997**, *48*, 353.
(130) Bristol-Myers Squibb, 2003, http://packageinserts.bms.com/pi/pi_taxol.pdf.
(131) National Cancer Institute, 2012, http://www.cancer.gov/cancertopics/druginfo/docetaxel.
(132) Schiff, P. B.; Fant, J.; Horwitz, S. B. *Nature* **1979**, *277*, 665.
(133) Jordan, M. A.; Toso, R. J.; Wilson, L. *Proc. Natl. Acad. Sci. U.S.A.* **1993**, *90*, 9552.
(134) Ojima, I.; Kuduk, S. D.; Chakravarty, S.; Ourevitch, M.; Bégué, J.-P. *J. Am. Chem. Soc.* **1997**, *119*, 5519.
(135) Georg, G. I.; Harriman, G. C. B.; Vander Velde, D. G.; Boge, T. C.; Cheruvallath, Z. S.; Datta, A.; Hepperle, M.; Park, H.; Himes, R. H.; Jayasinghe, L. In *Taxane Anticancer Agents: Basic Science and Current Status*; ACS Symposium Series 583; Georg, G. I., Chen, T. T., Ojima, I., Vyas, D. M., Eds.; American Chemical Society: Washington, D.C., 1995; p 217.
(136) Guéritte-Voegelein, F.; Mangatal, L.; Guénard, D.; Potier, P.; Guilhem, J.; Cesario, M.; Pascard, C. *Acta Crstallogr.* **1990**, *C46*, 781.
(137) Williams, H. J.; Scott, A. I.; Dieden, R. A.; Swindell, C. S.; Chirlian, L. E.; Francl, M. M.; Heerding, J. M.; Krauss, N. E. *Can. J. Chem.* **1994**, 252.
(138) Williams, H. J.; Scott, A. I.; Dieden, R. A.; Swindell, C. S.; Chirlian, L. E.; Francl, M. M.; Heerding, J. M.; Krauss, N. E. *Tetrahedron* **1993**, *49*, 6545.
(139) Vander Velde, D. G.; Georg, G. I.; Grunewald, G. L.; Gunn, C. W.; Mitscher, L. A. *J. Am. Chem. Soc.* **1993**, *115*, 11650.
(140) Mastropaolo, D.; Camerman, A.; Luo, Y.; Brayer, G. D.; Camerman, N. *Proc. Natl. Acad. Sci. U.S.A.* **1995**, *92*, 6920.
(141) Paloma, L. G.; Guy, R. K.; Wrasidlo, W.; Nicolaou, K. C. *Chem. Biol.* **1994**, *2*, 107.
(142) Gottesman, M. M.; Fojo, T.; Bates, S. E. *Nat. Rev. Cancer* **2002**, *2*, 48.
(143) Ojima, I.; Slater, J. C.; Michaud, E.; Kuduk, S. D.; Bounaud, P.-Y.; Vrignaud, P.; Bissery, M.-C.; Veith, J.; Pera, P.; Bernacki, R. J. *J. Med. Chem.* **1996**, *39*, 3889.
(144) Ojima, I.; Chen, J.; Sun, L.; Borella, C.; Wang, T.; Miller, M.; Lin, S.; Geng, X.; Kuznetsova, L.; Qu, C.; Gallagher, G.; Zhao, X.; Zanardi, I.; Xia, S.; Horwitz, S.; Clair, J. S.; Guerriero, J.; Bar-Sagi, D.; Veith, J.; Pera, P.; Bernacki, R. *J. Med. Chem.* **2008**, *51*, 3203.
(145) Ojima, I.; Wang, T.; Miller, M. L.; Lin, S.; Borella, C. P.; Geng, X.; Pera, P.; Bernacki, R. J. *Bioorg. Med. Chem. Lett.* **1999**, *9*, 3423.
(146) Ojima, I.; Kuduk, S.; Slater, J.; Gimi, R.; Sun, C.-M. *Tetrahedron* **1996**, *52*, 209.
(147) Kuznetsova, L. V.; Pepe, A.; Ungureanu, I. M.; Pera, P.; Bernacki, R. J.; Ojima, I. *J. Fluorine Chem.* **2008**, *129*, 817.
(148) Ojima, I.; Slater, J. C. *Chirality* **1997**, *9*, 487.
(149) Gut, I.; Ojima, I.; Vaclavikova, R.; Simek, P.; Horsky, S.; Linhart, I.; Soucek, P.; Knodrova, E.; Kuzetsova, L.; Chen, J. *Xenobiotica* **2006**, *36*, 772.
(150) Vuilhorgne, M.; Gaillard, C.; Sanderlink, G. J.; Royer, I.; Monsarrat, B.; Dubois, J.; Wright, M. In *Taxane Anticancer Agents: Basic Science and Current Status*; ACS Symposium Series 583; Georg, G. I., Chen, T. T., Ojima, I., Vyas, D. M., Eds.; American Chemical Society: Washington, D.C., 1995; p 98.
(151) Kuznetsova, L.; Sun, L.; Chen, J.; Zhao, X.; Seitz, J.; Das, M.; Li, Y.; Veith, J.; Pera, P.; Bernacki, R.; Xia, S.; Horwitz, S.; Ojima, I. *J. Fluorine Chem.* **2012**, *143*, 177.
(152) Pepe, A.; Kuznetsova, L.; Sun, L.; Ojima, I. In *Fluorine in Medicinal Chemistry and Chemical Biology*; Ojima, I., Ed.; Wiley-Blackwell: Chichester, 2009; p 117.
(153) Li, Y.; Poliks, B.; Cegelski, L.; Poliks, M.; Gryczynski, Z.; Piszcek, G.; Jagtap, P. G.; Studelska, D. R.; Kingston, D. G. I.; Schaefer, J.; Bane, S. *Biochemistry* **2000**, *39*, 281.
(154) Geney, R.; Sun, L.; Pera, P.; Bernacki Ralph, J.; Xia, S.; Horwitz Susan, B.; Simmerling Carlos, L.; Ojima, I. *Chem. Biol.* **2005**, *12*, 339.
(155) Rao, S.; He, L.; Chakravarty, S.; Ojima, I.; Orr, G. A.; Horwitz, S. B. *J. Biol. Chem.* **1999**, *274*, 37990.
(156) Nogales, E.; Wolf, S. G.; Downing, K. H. *Nature* **1998**, *391*, 199.
(157) Paik, Y.; Yang, C.; Metaferia, B.; Tang, S.; Bane, S.; Ravindra, R.; Shanker, N.; Alcaraz, A. A.; Johnson, S. A.; Schaefer, J.; O'Connor, R. D.; Cegelski, L.; Snyder, J. P.; Kingston, D. G. I. *J. Am. Chem. Soc.* **2007**, *129*, 361.
(158) Lowe, J.; Li, H.; Downing, K. H.; Nogales, E. *J. Mol. Biol.* **2001**, *313*, 1045.
(159) Sun, L.; Simmerling, C.; Ojima, I. *ChemMedChem* **2009**, *4*, 719.
(160) Ojima, I.; Kuznetsova, L. V.; Sun, L. In *Current Fluoroorganic Chemistry. New Synthetic Directions, Technologies, Materials and Biological Applications*; ACS Symposium Series 949; Soloshonok, V., Mikami, K., Yamazaki, T., Welch, J. T., Honek, J., Eds.; American Chemical Society/Oxford University Press: Washington, DC, 2007; p 288.
(161) Jaracz, S.; Chen, J.; Kuznetsova, L.; Ojima, I. *Bioorg. Med. Chem.* **2005**, *13*, 5043.
(162) Farokhzad, O. C.; Cheng, J.; Teply, B. A.; Sherifi, I.; Jon, S.; Kantoff, P. W.; Richie, J. P.; Langer, R. *Proc. Natl. Acad. Sci. U.S.A.* **2006**, *103*, 6315.
(163) Chu, T. C.; Marks, J. W., III; Lavery, L. A.; Faulkner, S.; Rosenblum, M. G.; Ellington, A. D.; Matthew Levy, M. *Cancer Res.* **2006**, *66*, 5989.
(164) Ducry, L.; Stump, B. *Bioconjugate Chem* **2010**, *21*, 5.
(165) Xia, W.; Low, P. *J. Med. Chem.* **2010**, *53*, 6811.
(166) Ojima, I.; Zuniga, E.; Berger, W.; Seitz, J. *Future Med. Chem.* **2012**, *4*, 33.
(167) Cobb, S.; Murphy, C. *J. Fluorine Chem.* **2009**, *130*, 132.
(168) Reivich, M.; Kuhl, D.; Wolf, A.; Greenberg, J.; Phelps, M.; Ido, T.; Casella, V.; Fowler, J.; Hoffman, E.; Alavi, A.; Som, P.; Sokoloff, L. *Circ. Res.* **1979**, *44*, 127.
(169) Ametamey, S.; Honer, M.; Schubiger, P. *Chem. Rev.* **2008**, *108*, 1501.
(170) Kimura, Y.; Simeon, F.; HAtazawa, J.; Mozley, P.; Pike, V.; Innis, R.; Fugita, M. *Eur. J. Nucl. Med. Mol. I* **2010**, *37*, 1943.
(171) Meyer, B.; Mann, N.; Lewis, J.; Milligan, G.; Sinclair, A.; Howe, P. *Lipids* **2003**, *38*, 391.
(172) Sauer, L.; Dauchy, R.; Blask, D. *Cancer Res.* **2000**, *60*, 5289.
(173) Grammatikos, S.; Subbaiah, P.; Victor, T.; Miller, W. *Br. J. Cancer* **1994**, *70*, 219.
(174) Bradley, M.; Webb, N.; Anthony, F.; Devanesan, P.; Wittman, P.; Hemamalini, S.; Chander, M.; Baker, S.; He, L.; Horowitz, S.; Swindell, C. *Clin. Cancer Res.* **2001**, *7*, 3229.
(175) Seitz, J.; Ojima, I. In *Drug Delivery in Oncology - From Research Concepts to Cancer Therapy*; Kratz, F., Senter, P., Steinhagen, H., Eds.; Wiley-VCH: Weinheim, 2011; Vol. 3, p 1323.
(176) Sparreboom, A.; Wolff, A.; Verweij, J.; Zabelina, Y.; van Zomeren, D. M.; McIntire, G.; Swindell, C.; Donehower, R.; Baker, S. *Clin. Cancer Res.* **2003**, *9*, 151.
(177) Kuznetsova, L.; Chen, J.; Sun, X.; Wu, A.; Pepe, J.; Veith, P.; Pera, R.; Bernacki, R.; Ojima, I. *Bioorg. Med. Chem. Lett.* **2006**, *16*, 974.
(178) Chen, J.; Jaracz, S.; Zhao, X.; Chen, S.; Ojima, I. *Expert Opin. Drug Deliv.* **2005**, *2*, 873.
(179) Chari, R. V. J. *Adv. Drug Delivery Rev.* **1998**, *31*, 89.
(180) Doronina, S. O.; Mendelsohn, B. A.; Bovee, T. D.; Cerveny, C. G.; Alley, S. C.; Meyer, D. L.; Oflazoghu, E.; Toki, B. E.; Sanderson, R. J.; Zabinski, R. F.; Wahl, A. F.; Senter, P. D. *Bioconjugate Chem.* **2006**, *17*, 114.
(181) Beck, A.; Haeuw, J. F.; Wurch, T.; Goetsch, L.; Bailly, C.; Corvaia, N. *Discov. Med.* **2010**, *10*, 329.
(182) Ojima, I.; Geng, X.; Wu, X.; Qu, C.; Borella, C.; Xie, H.; Wilhelm, S.; Leece, B.; Bartle, L.; Goldmacher, V.; Chari, R. *J. Med. Chem.* **2002**, *45*, 5620.
(183) Kigawa, J.; Minagawa, Y.; Kanamori, Y.; Itamochi, H.; Cheng, X.; Okada, M.; Oisho, T.; Terakawa, N. *Cancer* **1998**, *82*, 697.
(184) Chen, J.; Chen, S.; Zhao, X.; Kuznetsova, L.; Wong, S.; Ojima, I. *J. Am. Chem. Soc.* **2008**, *130*, 16778.

(185) Ojima, I. *Acc. Chem. Res.* **2008**, *41*, 108.
(186) Chen, S.; Zhao, X.; Chen, J.; Chen, J.; Kuznetsova, L.; Wong, S.; Ojima, I. *Bioconjugate Chem.* **2010**, *21*, 979.
(187) Russell-Jones, G.; McTavish, K.; McEwan, J.; Rice, J.; Nowotnik, D. *J. Inorg. Biochem.* **2004**, *98*, 1625.
(188) Leamon, C. P.; Reddy, J. A. *Adv. Drug Delivery Rev.* **2004**, *56*, 1127.
(189) Zempleni, J. *Ann. Rev. Nutr.* **2005**, *25*, 175.
(190) Zempleni, J.; Wijeratne, S.; Hassan, Y. *Biofactors* **2009**, *35*, 36.
(191) Bianco, A.; Kostarelos, K.; Prato, M. *Curr. Opin. Chem. Biol.* **2005**, *9*, 674.
(192) Prato, M.; Kostarelos, K.; Bianco, A. *Acc. Chem. Res.* **2008**, *41*, 60.
(193) Gillies, E.; Frechet, J. *Drug Discov. Today* **2005**, *10*, 35.
(194) Gaertner, H.; Cerini, F.; Kamath, A.; Rochat, A.-F.; Siegrist, C.-A.; Menin, L.; Hartley, O. *Bioconjugate Chem.* **2011**, *22*, 1103.